A Process with Decoupled Absorber Kinetics and Solvent Regeneration through Membrane Dewatering and In-Column Heat Transfer

Final Technical Report

Reporting Period:
May 1, 2018 to February 28, 2022

Principal Authors:
Reynolds Frimpong, Kunlei Liu and Lisa Richburg

Contributing Authors (in alphabetical order):
Bradley Irvin, James Landon and Feng Zhu
University of Kentucky, Lexington, KY

Report Issued
April 25, 2022

Work Performed Under Award Number
DE-FE0031604

SUBMITTED BY
University of Kentucky Research Foundation
109 Kinkead Hall, Lexington, KY 40506-0057

PRINCIPAL INVESTIGATOR
Kunlei Liu
+1-859-257-0293
kunlei.liu@uky.edu

DOE PROGRAM MANAGER
David Lang
David.Lang@netl.doe.gov
+1-412-386-4881

SUBMITTED TO
U.S. Department of Energy National Energy Technology Laboratory

ACKNOWLEDGEMENT: This material is based upon work supported by the Department of Energy under Award Number DE-FE0031604. University of Kentucky Center for Applied Energy (UK CAER) is grateful to the U.S. Department of Energy National Energy Technology Laboratory for the support of this project. UK CAER is also grateful to our project partners Lawrence Livermore National Laboratory (LLNL), Media & Process Technology (MPT), ALL4 LLC and Trimeric Corporation. The specific assistance of Du T. Nguyen (LLNL); Rich Ciora, Doug Parsley, Amy Chen (MPT); Clay Whitney, Nicholas Konefal and Stewart McCollam (ALL4 LLC) is greatly appreciated.

The project team is also grateful to the many UK CAER research personnel for their assistance and various contributions to the project, as listed below.

Keemia Abad
John Adams
Saloni Bhatnagar
Jacob Blake
Jonathan Bryant
Darby Campbell
Landon Caudill
Shanice Edwards
Zhen Fan
James Fussinger
Len Goodpaster
Ryan Hines
Otto Hoffmann
Marshall Marcum
Roger Perrone
Aaron Smith
Steve Summers
John Taylor
Jesse Thompson
Shino Toma
Jinwen Wang
Evan Williams

ABSTRACT

This report summarizes the work conducted on project DE-FE0031604 where University of Kentucky Center for Applied Energy (UK CAER) has validated its intensified CO_2 capture process through substantial enhancements to the kinetics of the absorption process and energy reductions by absorber temperature profile modification, dewatering and heat integration technologies for achieving significant capital and operating cost reductions.

To address DOE's objective of improving post-combustion CO_2 capture technology and reducing associated cost, UK CAER employed an intensified process which combined three key aspects targeted at overcoming inherent limitations or barriers in the conventional CO_2 capture and desorption process. The process designed to be independent of the type of solvent used, included (1) the use of 3-D printed two-channel structured packing material to control the temperature profile and increase the CO_2 absorption rate in the absorber, (2) a zeolite membrane dewatering unit for dewatering of the carbon-rich solvent to decouple solvent concentration needs for CO_2 absorption and desorption, and (3) a rich-split feed with two-phase flow heat transfer prior to the stripper that provided a secondary point of vapor generation to provide energy savings in steam extraction and solvent regeneration.

The project was executed over two budget periods. This involved testing of individual process components which included the advanced heat transfer packing and the dewatering membrane on UK CAER's 30 liter per minute (L/min) CO_2 (3" Column) capture bench unit with simulated flue gas in the first budget period. Subsequent scaled-up testing of these components together with the split-feed configuration were also tested in UK CAER's 0.1 MWth CO_2 capture unit with coal-derived flue gas in the second-budget period. Long term studies were done during this period to assess process and solvent performance over extended duration. Project partners Lawrence Livermore National Laboratory (LLNL) and Media & Process Technology (MPT) led the development efforts for the advanced packing material and dewatering membrane respectively. Data from the long term testing was used as input for an environmental, health and safety (EH&S) assessment for the process and scaled technology performed by ALL4 LLC. Trimeric Corporation also completed a techno-economic analysis (TEA) for the UK CAER technology which was compared to the DOE reference Case B12B.

Tests on the 3" column capture unit showed that the advanced heat transfer packing could be used to lower the bulge temperature in the absorber, and this was also proven in the scaled testing in the 0.1 MWth CO_2 capture unit. The bulge temperature could be lowered by >10 °C, changing the temperature profile in the absorber, and showed potential to enhance absorption with the ability to tailor the profile to provide conditions suitable for a solvent's properties and kinetics. Conditions for short term evaluation of a 19" zeolite dewatering membrane on the 3" column capture unit yielded desirable fluxes and sustained rejection rates of >80%. However, for the scaled testing of six membrane modules consisting of 21 parts of 31-inch-long membrane tubes in each bundle (surface area 0.3 m^2), over a more extended duration, similar rejection rates could not be achieved. With the split-feed of the rich stream to the stripper, improved heat recovery minimized waste heat exiting the top of the stripper. The stripper exhaust temperatures could be reduced by >10 °C; reducing the amount of water vaporization contributed to lowering the regeneration energy by ~ 15%. The energy benefit could be sustained from the long term monitoring of the solvent

performance. The solvent properties were not significantly impacted over the long-term operations.

The benefits of the UK CAER process demonstrated experimentally were mostly validated from the TEA comparing a commercial scale application of the technology to DOE reference Case B12B. The cost of CO_2 capture for the UK CAER technology was estimated to be ~$34.97/tonne of CO_2 captured; a reduction of 23% compared to Case B12B. The increase in cost of electricity was also shown to be 16% lower than that of Case B12B. The total parasitic demand was also shown to be 11% lower. The key drivers for the benefits are a result of the process intensification approaches employed in the UK CAER technology for enhanced solvent performance, effective heat recovery and improved energy performance. The EH&S assessment did not find any major environmental concerns or barriers to the full scale implementation of the technology.

Table of Contents

1 PROJECT SUMMARY

1.1 Executive Summary

Project Description

With the support of the DOE under award DE-FE0031604, a project team, led by the University of Kentucky Center for Applied Energy (UK CAER), in collaboration with Lawrence Livermore National Laboratory (LLNL), Media & Process Technology (MPT), Trimeric Corporation, and ALL4 LLC (formerly Smith Management Group) completed a study to demonstrate benefits of a solvent-independent intensified process for CO_2 capture in UK CAER's post-combustion CO_2 capture bench units with corresponding techno-economic analysis (TEA) and environmental, health and safety (EH&S) assessment, as well as technology gap analysis. The integrated process consisted of a temperature profile modified absorber, a membrane dewatering unit, and a multiple-feed pressurized stripper working in tandem to reduce the operating and capital costs associated with CO_2 capture. This was achieved with the fabrication and installation of heat transfer structured packing and dewatering membrane modules and retrofitting of the 0.1 MWth CO_2 capture unit for multiple feeds to the stripper for the full evaluation of the intensified process.

The project employed three key process intensification approaches geared towards addressing critical hurdles in conventional post-combustion CO_2 capture (PCCC). This included the use of (i) a 3-D printed heat transfer packing in the top section of the absorber to control the temperature profile in the absorber to enhance CO_2 absorption in the solvent and in effect reduce the absorber size; (ii) a zeolite-based membrane dewatering unit to decouple solvent concentration for absorption and desorption; and (iii) an additional two-phase flow heat transfer prior to the stripper providing a secondary point of vapor injection into the stripper, which allowed solvent regeneration to be performed with lower steam extraction with consequent energy savings for the capture process and ultimately increase power generation for power plants.

Project Goals

The objectives of the project were to research the intensified process on UK CAER's post-combustion CO_2 capture bench units using both simulated and coal-derived flue gas which required the fabrication of additional components and retrofitting the units. As part of this effort, design specifications and locations for the in-situ heat transfer packing material installed in the absorber, and the heat-exchanger configuration for the stripper were determined. Membrane materials were developed and modules configured for the de-watering unit. The performance of the heat transfer packing material was initially evaluated in a 3" absorber column bench unit (simulated flue gas testing) and with design improvement on open area for subsequent evaluation in the 0.1 MWth CO_2 capture unit (4" absorber column) for overall evaluation of all components of the intensified process with coal-derived flue gas. The long-term study performed was used to assess material and operational stability.

The project was performed over two budget periods as follows:

Budget Period 1: In the first budget period, individual process components were tested on UK CAER's 30 liter per minute (L/min) CO_2 (3" Column) capture bench unit with advanced packing material placed in the absorber column, and a dewatering membrane module installed after the lean/rich (L/R) heat exchanger (HXER) before the stripper. The experimental findings were used to inform modifications on packing design and membrane configuration for subsequent testing in UK CAER's 0.1 MWth CO_2 capture unit.

Budget Period 2: In the second budget period, the 0.1 MWth bench-scale CO_2 capture unit was retrofitted with advanced packing, a dewatering membrane module, and an additional, high-end L/R heat exchanger placed between the dewatering membrane module and the stripper. Initial tests were performed to troubleshoot the new process components followed by parametric tests which culminated in a 1000-hour long-term campaign where the operational stability and energetic benefits of the process components were examined. A techno-economic analysis (TEA) and an environmental, health, and safety (EH&S) risk assessment of the process were also performed.

1.2 Success Criteria

The following success criteria established for the project were met as shown in **Exhibit 1.2.1**

Budget Period 1

- The peak absorber temperature could be reduced by >10 °C with the heat transfer packing material installed in the top section of the 3" absorber column.
- Zeolite Y membranes were developed with fluxes of >10 kg/m^2/h and rejection rates of >90%.
- Dewatering Zeolite Y Module design was completed with surface area of >200m^2/m^3.

Budget Period 2

- The stripper heat integration was demonstrated to provide an energy savings of >10% on the 0.1 MWth CO_2 capture unit.
- Heat transfer packing could lower the bulge temperature by >10 °C.
- A long-term energy savings of >15% from the 1000 hr study was achieved.
- The dewatering membrane packing density was increased to 322 m^2/m^3.
- An Aspen model for the entire integrated system was generated.
- TEA completed for the process showed an 11% reduction in the total parasitic demand, ~ 16% decrease in the increase of cost of electricity, and a 23% reduction in the cost of CO_2 capture when UK CAER capture technology is compared with DOE reference Case B12B. The total plant cost was also reduced by ~44%.
- EH&S assessment completed identified no direct extremely hazardous substances with the materials used in the process and there were no major concerns detrimental to the large scale implementation of the technology.

Exhibit 1.2.1. Success Criteria Satisfied

1.3 Other Findings and Challenges

Other key findings and challenges encountered in the project include:

- Liquid distribution underneath the in-situ heat transfer packing due to the temperature gradient in liquid film.
- The seal of membrane module due to thermal stress swings in the high pH working environment.
- The approach temperature at L/R HXERs outlet under various liquid circulation rates and carbon loading in the solvents due to the fixed size of HXERs.

2 BACKGROUND AND TECHNOLOGY DESCRIPTION

2.1 Project Objective and Background

Objectives

Developing transformative post-combustion CO_2 capture through

- Enhanced mass transfer for low capital via applying 3-D printed two-channel structured packing material to control/modify the absorber temperature profile for optimizing reaction kinetics and driving forces
- Lower regeneration energy via
  - Zeolite dewatering membrane unit capable of >15% dewatering of the carbon-rich solvent prior to the stripper
  - Two-phase flow heat transfer prior to the stripper providing a secondary point of vapor generation

Exhibit 2.1. Project Objectives.

To meet DOE's performance and cost targets for CO_2 capture, innovative approaches that provide a pathway for the realization of the goals have to be adopted. With technological improvements geared towards significant capital and operating cost reduction, energy savings and performance enhancements, the UK CAER intensified process for CO_2 capture was demonstrated with three main objectives as highlighted in **Exhibit 2.1.** First, a 3-D printed two-channel heat transfer structured packing installed in the top-section of the absorber with one channel for gas-solvent reaction, and another for heat rejection, is used to control the absorber temperature profile to optimize reaction kinetics and CO_2 driving force for improved solvent performance. The process enhancement will provide capital cost savings with a reduction of up to about 50% in absorber size. Secondly, a zeolite-dewatering membrane capable of >15% dewatering of the carbon-rich solvent prior to the stripper will allow more concentrated solvent to the stripper which will require lower energy consumption for regeneration. Third, a two-phase flow heat transfer prior to the stripper is used to provide a secondary point of vapor injection into the stripper which allows solvent regeneration with lower fresh steam extraction (lower regeneration energy) consequently resulting in greater power generation from steam turbines. An energy savings of ~15% is achievable in the regeneration energy in the stripper.

The process enhancements were demonstrated on UK CAER's 3" bench (with simulated flue gas) and the 0.1 MWth CO_2 capture unit (with coal-fired flue gas) with experimental information

gathered serving as inputs for EH&S assessment by ALL4 LLC and a TEA by Trimeric Corporation. The heat transfer packing materials used were based on manufacturing techniques developed and designed by project partner LLNL, and work on the dewatering zeolite membranes modules was in close partnership with MPT. The intensified process and each of the individual components are applicable to any solvent-based post-combustion CO_2 capture including coal-based and natural gas electricity generating plants where heat integration and enhancement processes are of paramount necessity for improved efficiencies. The project, as a whole, can readily be demonstrated at commercial-scale with the relative straightforward piping, packing, and heat integration modifications required.

2.2 Process Description

The intensified process as previously noted has three areas of process enhancements which can readily be assimilated into the conventional or any solvent-based post-combustion CO_2 capture process. UK CAER's CCS technology (demonstrated on a 0.7 MWe pilot-scale at E.W. Brown Generating Station, Harrodsburg, KY previously under DOE Project DE-FE0007395) uniquely uses an additional stripper compared with the conventional in a two-stage stripping process with additional heat recovery schemes for improved performance in the capture process. Building on the demonstrated gains, the process enhancements described here will further advance the technology.

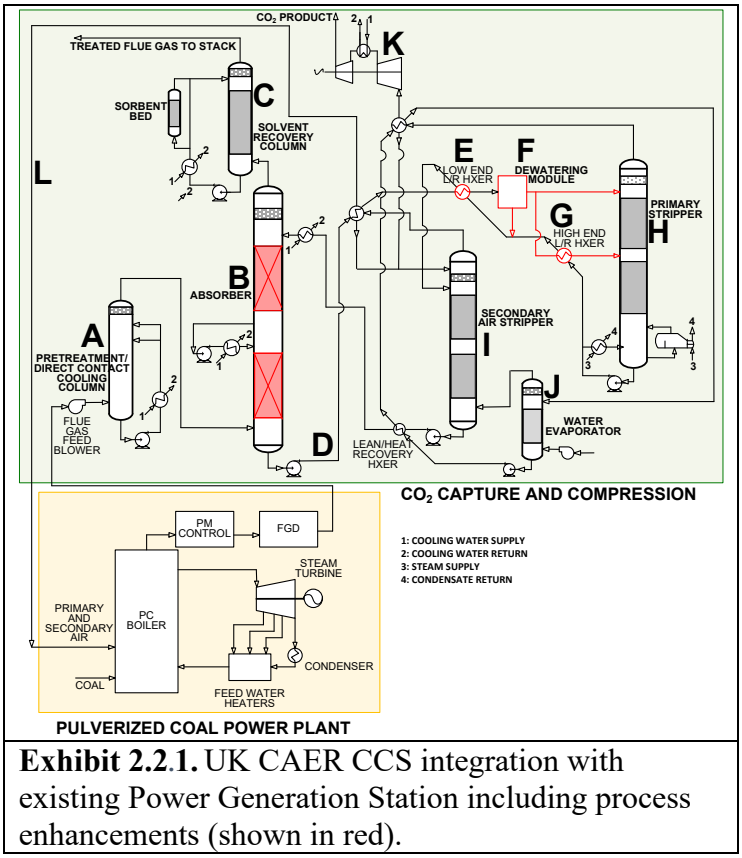

Exhibit 2.2.1. UK CAER CCS integration with existing Power Generation Station including process enhancements (shown in red).

A summary of integration of the process intensified UK CAER CCS into an existing commercial-scale power plant (RC B12B) is shown in **Exhibit 2.2.1.** The UK CAER CCS and compression block comprises a pretreatment tower, a packed CO_2 absorber with an embedded heat-transfer unit, a 3-D discretized packing arrangement, a water-wash section connected to a sorbent bed, two packed stripper columns, a reboiler, a reclaimer, heat exchangers including both low and high end heat exchangers prior to the stripper, pumps, filtration devices, auxiliary equipment, and a multi-stage compressor with intercoolers.

In detail, flue gas enters a booster fan followed by a counter-flow pre-treatment/direct cooling tower (A) for additional SO_2 polishing in order to minimize solvent degradation and potential membrane fouling. The polished flue gas then enters the CO_2 absorber (B) with three sections of discretized packing for CO_2 capture with one embedded heat transfer unit at the top. The CO_2 depleted flue gas exiting the absorber passes through a water-wash column (C) to capture amine aerosols before being emitted. After gaseous CO_2 is transferred to the liquid phase, the carbon-rich solution (D) exits the absorber, is pressurized, passes through a heat recovery unit [secondary stripper overhead condenser] and the low end L/R HXER (E), and is dewatered (F). The amine-concentrated stream is split with 20-50% of the total rich flow entering the top of the stripper at about 180 °F (solvent and stripping dependent). The remaining rich flow is heated further in the high end L/R HXER (G), resulting in a two-phase flow, with 2-6 wt% vapor entering the middle of the stripper at about 200-250 °F. The primary, steam-driven stripper is operated at about 45 psi (3 bar) (H). If the RC B12B steam condition is maintained for the CCS, the extracted steam will flow directly to a high-temperature feed water heater (FWH) in parallel with FWH 5 and FWH 6 for exergy recovery prior to feeding the reboiler. The water saturated air stream used in the secondary stripper (I) is generated in a water evaporator (J) as part of the heat recovery loop. After exiting the heat recovery unit, the CO_2 product stream is pressurized to 2200 psi (153 bar) with intercooling for downstream utilization/sequestration (K). Heat is recovered from the carbon-lean solution exiting the primary stripper with the carbon rich solution in both the high end (G) and low end (E) L/R HXERs. The lean solution is then sent to the top of an ambient pressure air-swept, packed secondary stripper (I) to further reduce the carbon loading prior to cooling, and then, returning the solution to the absorber (B). The CO_2-laden air exiting the secondary stripper (8-10% CO_2, dry basis), is fed to the boiler as secondary combustion air (L).

2.3 Overview of Technology

The intensified process addresses three critical hurdles for post-combustion CO_2 capture which includes the (1) unfavorable temperature profiles in the absorber (2) contradictory effects of solvent concentrations in the absorber and stripper, and (3) single point of vapor generation in the stripper.

1. Heat-Transfer Structured Packing

Under-utilized Absorber Due to Temperature Bulge:
The diameter of an absorption/desorption column is generally determined by the flooding point at a given L/G ratio. The highest flooding potential for a fast-reacting solvent occurs at the temperature bulge, which typically occurs in the top packing section of the column, ~10-15% of packing height from the top. A characteristic temperature profile is shown for the 0.7 MWe small-

pilot capture unit for an L/G of 3.2 in **Exhibit 2.3.1.** A temperature rise of ~50 °F is observed ~10 feet below the lean amine feed. The temperature bulge represents an imbalance in the CO_2 absorption rate (releasing heat) and the heat rejection via evaporation and convection during the reaction between solvent and CO_2. To flatten the temperature profile and lower the capital cost, a Discretized Packing Arrangement (DPA) with in-situ heat transfer surfaces is employed to control the reaction of CO_2 absorption to balance the heat release (from CO_2 capture) with heat rejection (water evaporation and sensible heat change).

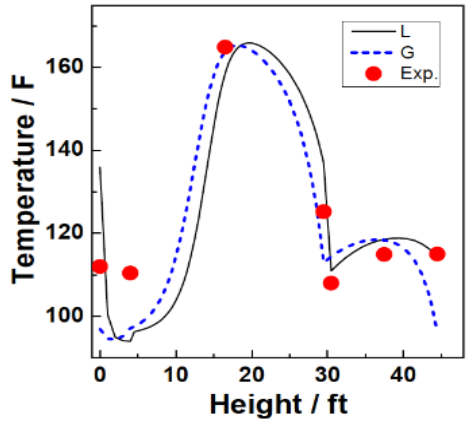

Exhibit 2.3.1. 0.7 MWe small pilot absorber temperature profiles (model prediction for liquid (L) and Gas (G) – solid lines, experimental data in red dots).

The upper section will contain high capacity, low efficiency 3-D printed two-channel packing to reduce the CO_2 absorption (less heat released). Additionally, coolant will be deployed to reject heat. The middle section will contain high efficiency, high capacity packing to boost the CO_2 reaction with solvent. The bottom section will contain low capacity, high efficiency packing to counter potential channel flow caused by higher viscosity and surface tension. This approach can be used to manage the absorber diameter and height to offer significant reduction in capital cost.

2. Dewatering Membrane

Conflicting Requirements for Solvent Concentration between the Absorber and Stripper: It is well accepted that the absorber is mass transfer/diffusion-controlled while the stripper is equilibrium-controlled. For the equilibrium-controlled stripper, the carbon loading via CO_2 partial pressure will determine the size of the stripper as well as the energy associated with stripping gases, which typically accounts for approximately 40% of the overall energy required for solvent regeneration. Higher solvent concentrations typically produce higher carbon loadings per kilogram solution at a given temperature compared to a diluted solvent, so it would be preferable for stripper applications. However, higher solvent concentrations always correspond to higher viscosities. For a diffusion-controlled absorber using any advanced fast solvent, the mass transfer coefficient (K_G) is dominated by the resistance from the chemical reaction of CO_2 and amine in the reaction film and diffusion of unreacted amine and carbamate between reaction interface and bulk. Unfortunately, the diffusivity between the reaction interface and the bulk is determined by the Stokes-Einstein equation $\left(D_{CO_2}\right)_{\text{amine soln}} = \left(D_{CO_2}\right)_{\text{water}} \left(\frac{\eta_{\text{water}}}{\eta_{\text{amine soln}}}\right)^{0.8}$, where high viscosity will increase the diffusion resistance, thereby reducing mass transfer. In an attempt to overcome this contradiction, a dewatering membrane is installed in the rich solvent stream line prior to the stripper. During operation, approximately 15% of the water will be permeated through the membrane and then returned to the absorber, leaving a carbon concentrated solution entering the stripper for

regeneration and resulting in lower energy consumption while not impacting CO_2 absorption rates in the absorber.

3. Multiple-feed to Stripper

Under-utilized and Inefficient Stripper: In the conventional stripping process, the reboiler uses extracted steam to evaporate water in the solvent (a) as a carrier gas to strip CO_2 out of the solvent and (b) as an energy carrier to heat the stripper to a desired temperature(s) as required by the solvent and stripper operating pressure. During this process, significant exergy is lost. Secondly, high rich solvent temperature entering the stripper prevents the gaseous phase from condensing at the top of the stripper, reducing heat recovery within the system as more water vapor is lost with the gaseous exhaust. Consequentially, the typical temperature and product CO_2 flow have been observed as plotted in **Exhibit 2.3.2.** The UK CAER experimentally verified Aspen model was used to generate the stage-level CO_2 and H_2O flows shown on the right in this figure. It clearly indicates that almost all of the CO_2 was liberated from the solvent at the bottom half of stripper as illustrated by a flat plateau on the temperature profile, and the CO_2 flowrate from the top of stripper packing to 14 ft for a stripper equipped with a total of 30 ft of structured-packing.

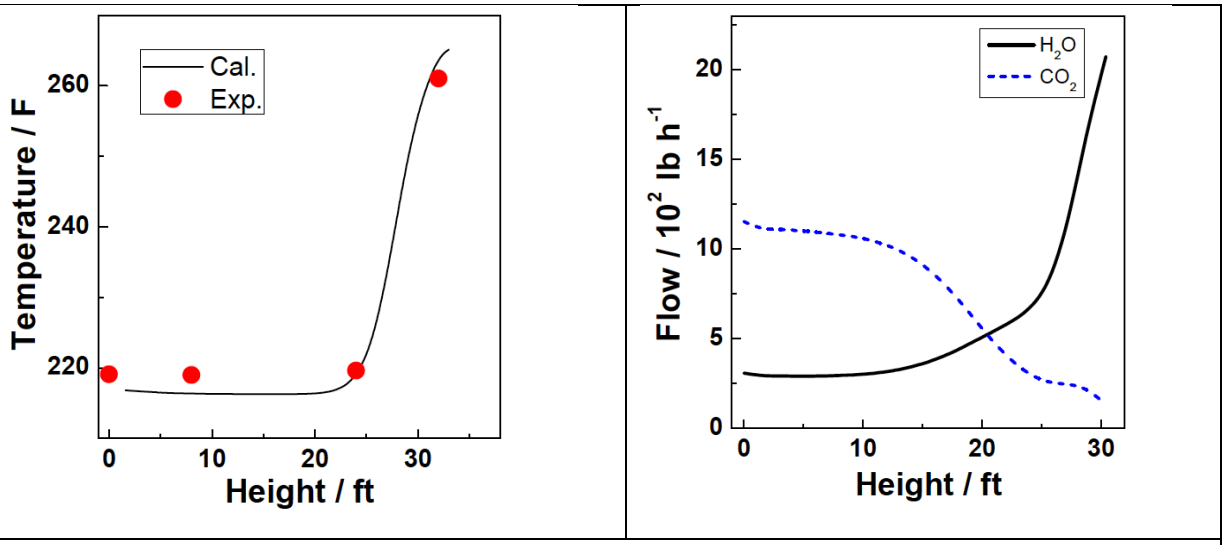

Exhibit 2.3.2. Liquid temperature (left, experimental data red dots) and CO_2-H_2O fluxes (right, water with black line and CO_2 with blue dashed line) based on UK CAER's 0.7 MWe post-combustion CO_2 capture pilot facility.

To minimize the complications associated with multiple vapor generation points, UK CAER has developed the use of a multi-point rich solvent feed by dividing the traditional lean/rich (L/R) heat exchanger into two sections – a low-end L/R HXER and a high-end L/R HXER (a second source for vapor generation). The feed to the primary stripper is then split into two streams: (A) After the low-end L/R HXER, 20-50% of the total rich flow with a temperature (typically around 180 °F, but depends on the solvent and the stripper operating pressure) is fed to the top of stripper packing as a heat sink to condense water vapor and subsequently reduce the H_2O/CO_2 ratio. (B) The remaining rich flow will be further heated through the high-end L/R HXER so that two phase flow is achieved with 2-6 wt% vapor entering the middle of the stripper packing at a temperature around

110 to 125 °C. This vapor will act as a secondary source of carrier gas for CO_2 stripping. UK CAER modelling indicates the H_2O/CO_2 ratio in the stripper exhaust will be significantly reduced from 0.8-1.0, conventionally, to 0.3-0.4, resulting in a ~26% reduction in steam consumption.

3 DESIGN OF 3-D PRINTED PACKING FOR ABSORBER

The unfavorable temperature profile in the absorption column results in the under-utilization of the absorber and limits solvent performance. When this is properly managed enhanced absorption rates as well as effective maximization of the absorber diameter and height can be realized. A direct conflict exists between the CO_2 absorption rate and the gas/liquid local temperature. While the mass transfer coefficient, k_g', increases as the solvent temperature increases, the CO_2 driving force decreases due to a higher P^*_{CO2} in the solvent and a lower gas P_{CO2} due to higher water vapor pressure. A 3-D heat transfer packing is therefore used in the absorber for heat management to help achieve the desired temperature profiles for enhanced solvent performance. Suitable packing materials and configurations were identified, designed and fabricated using 3-D additive printing methods.

3.1 Material Identification and Testing

UK CAER in consultation with LLNL identified potential polymeric candidates that could be used for the packing. Some of the considerations included material compatibility with amine solvents and ease of printability. **Exhibit 3.1.1** shows the characteristics of some of the polymer candidates. The top section candidates could be printed readily by LLNL while those in the bottom section required some slight modifications to the printer.

Exhibit 3.1.1. Polymer candidates for 3-D heat transfer packing material.

Polymer	Current Printability	Printability Notes	Ethanolamine Compatibility
Acrylonitrile Butadiene Styrene	Yes	Easy	A for diethanolamine
Polystyrene	Yes		A for diethanolamine
High-density polyethylene	Yes		Some effects after 7 days of constant exposure at 50 °C
Copolyester	Yes	Easy	*likely similar to HDPE
Polycarbonates	Yes		B
Polypropylene	Yes		B
Polyphenylene sulfide	No	Requires hot, all-metal print head and hotter base plate	A
Polyether ether ketone	No		A for triethanolamine
Polyphenyl sulfone	No		A for polysulfone
Polyether Imide	No		*likely good resistance

*A represents outstanding stability in amine, B – reduced stability, may have chemical or structural changes over time.

Three candidates, acrylonitrile butadiene styrene (ABS), polystyrene (PS), and high-density polyethylene (HDPE) were subsequently tested for stability in CAER solvent. Test samples of ABS, PS, and HDPE provided by LLNL were immersed in the solvent for a period of >120 hours at an elevated temperature of 60 °C, representative of the temperature bulge reached without in-situ cooling in the absorber column in CAER's 0.1 MWth post-combustion CO_2 capture facility. Mass, volume, and color changes were tracked during this stability study. All three samples were found to be stable in the process solvent with no mass/volume changes and no visible changes in color. LLNL subsequently printed test packing using ABS, PS, and HDPE. A picture of ABS test samples is shown below in **Exhibit 3.1.2.** ABS and PS were 3D printed with minimal difficulty, but the HDPE sample did not adhere well to the build plate. ABS was selected as the material of choice for 3-D printing due to the ease of printing and stability in the solvent.

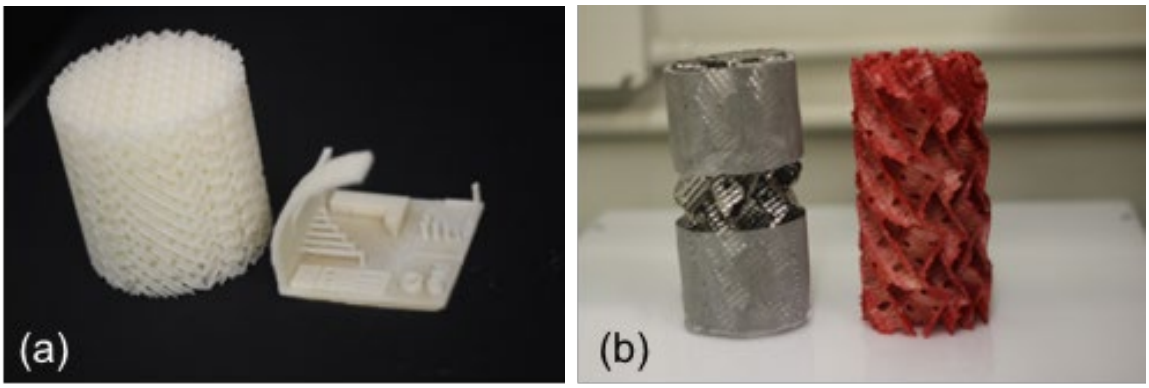

Exhibit 3.1.2. Images of 3D printed packing material using PS and ABS with (a) PS printed with 700Y design and (b) ABS printed 250Y design.

3.2 Packing Design and Fabrication

3-D printed heat transfer packing material was designed with the basis of >150 W of heat removal duty required. Using the 250Y packing configuration as an example, a 6-inch tall heat transfer unit was designed with 0.8 mm wall thickness, 3 mm fluid channel height, 66% open area, and 0.16 m^2 of surface area. The percent open area could be further increased to >85% by limiting the fluid channel height in the packing material and/or decreasing the number of fluid channels used for heat transfer.

A schematic of the designed heat transfer packing is shown in **Exhibit 3.2.1** along with a still image of water flowing through the first test print of the ABS heat transfer packing. During leak testing of this first test print, water flowed at up to 1 L/min through the fluid channel without any noticeable leaks. Acetone was used post-printing to further seal the fluid channels before leak testing. LLNL worked to increase the ABS density in certain locations before the addition of the manifold necessary to install into UK CAER's small CO_2 capture bench unit.

To characterize the wettability of the packing, contact angles for the 3-D printed ABS were measured in monoethanolamine (MEA) and compared to angle measurements for stainless steel. The contact angle was approximately 70° for ABS and 45° for stainless steel, meaning ABS is less hydrophilic (i.e., less wettability) compared to stainless steel. The contact angle for water on ABS

was also measured at 0 hours and after 217 hours in a blended amine solvent. The contact angle for water was approximately 83° before and after exposure to the blended amine solvent.

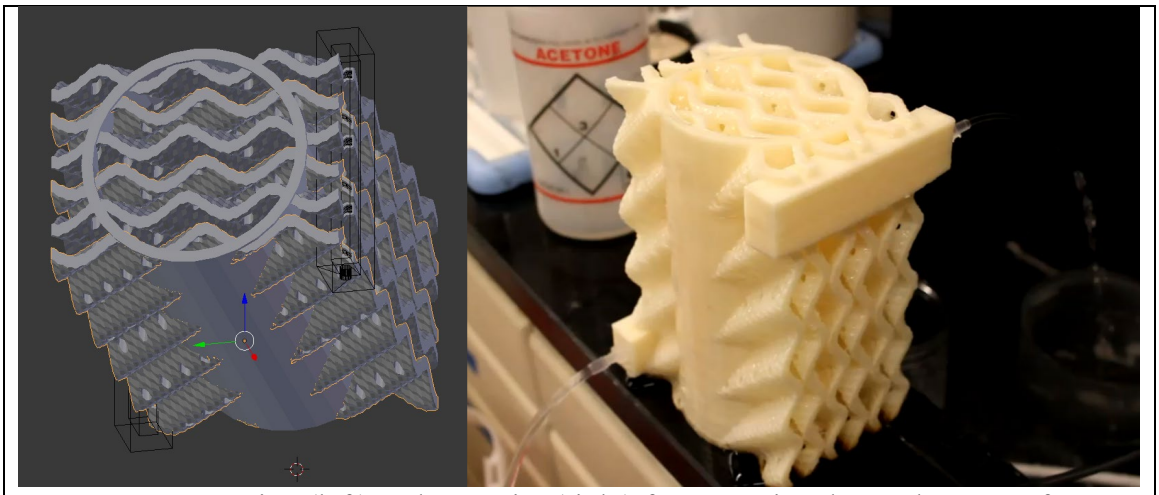

Exhibit 3.2.1. Design (left) and test print (right) for 3-D printed ABS heat transfer packing material based on 250Y design.

To limit leak-prone points created while printing circular geometries, alternative designs with 'cut-outs' were explored. The cut-outs are present to allow transfer of amine between sections of packing surface to increase gas-liquid mixing and redistribution. To replace the circular cut-out that was used in the previous packing design, a commercial structured packing, a diamond cut-out was proposed due to the continuity of deposited material available during the printing process. This higher level of continuity is achieved since the printing tip depositing the polymer would make limited return trips to the same location as opposed to a much greater number of return trips needed to accommodate a circular design. Heat transfer packing material based on the 250Y design and diamond cut-outs using acrylonitrile butadiene styrene (ABS) was therefore subsequently printed by LLNL as shown in **Exhibit 3.2.2**, and leak testing was conducted at up to 2 L/min. Flange sealing points were added to the top and bottom of the packing material to enable installation into UK CAER's 3" CO_2 capture unit.

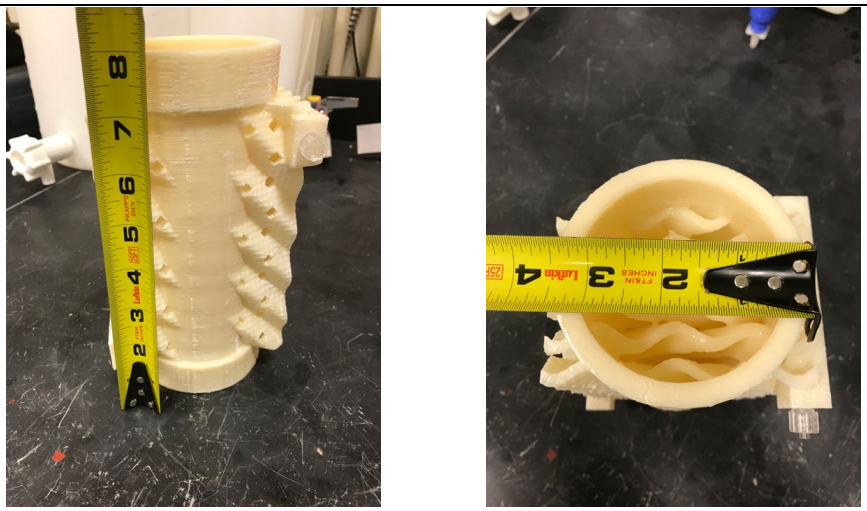

Exhibit 3.2.2. Heat transfer packing material from the side (left) and the top (right) using ABS material based on 250Y design with diamond cut-outs.

Working with modified designs from LLNL, a vendor, 3D Hubs fabricated the ABS 3-D printed packing for testing in the 3" CO_2 capture bench unit. Initial samples of packing which were fabricated using the FDM technique leaked. A resin was identified by 3D Hubs that had excellent compatibility with amine solvents, and together with using a stereolithography apparatus (SLA) instead, leak-free packing materials were obtained. A picture of one of the test prints using SLA is shown in **Exhibit 3.2.3**. Test prints immersed in the CAER amine solvent and examined for visible reaction, swelling, and discoloration showed no changes. However, the packing was found to be too brittle for practical implementation into the absorber column. Cracks developed on the wall once flanges were installed on the packing material and incorporated in the absorber column in UK CAER's 3" CO_2 capture bench unit.

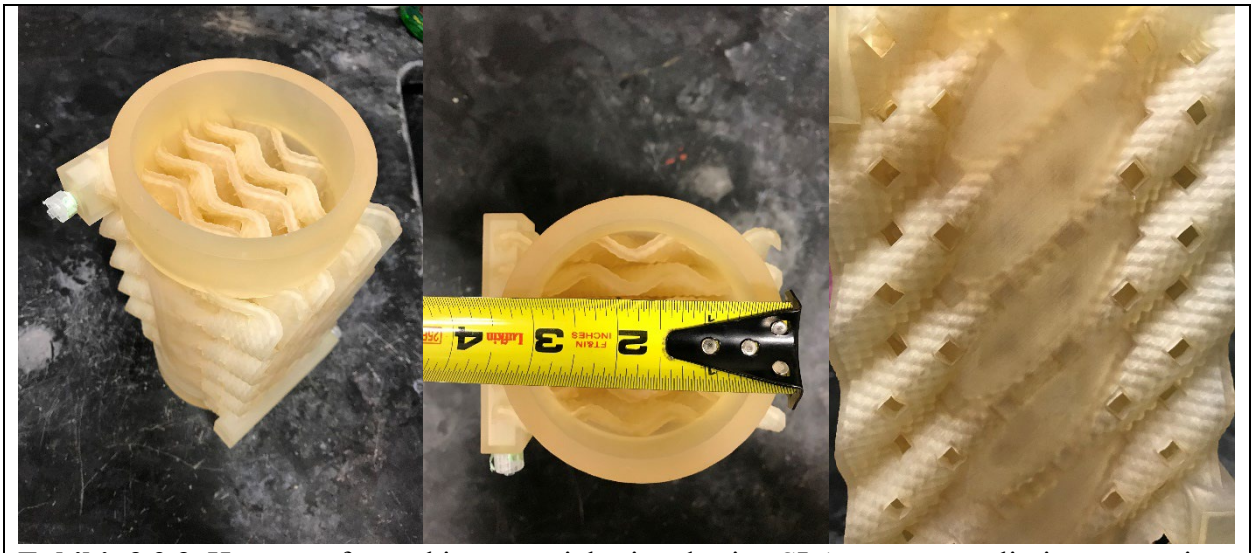

Exhibit 3.2.3. Heat transfer packing material printed using SLA process to eliminate porosity during the printing process.

In view of the challenges encountered with the printed packings described above, additional printing was carried out using a revised design file from LLNL. Stainless steel (316) packing was printed using a third party vendor, Protolabs, as shown in **Exhibit 3.2.4.** The revised design file included changes to the cooling access points to limit stress at those locations as well as confinement of the heat transfer channel design to inside the cylinder. A leak-free design was achieved using direct metal laser sintering (DMLS) with no post-processing. This packing material was subsequently installed in the 3" bench unit, and performance of in-situ cooling studies performed. The heat transfer coefficient for stainless steel (SS) is about 2 orders of magnitude higher than ABS (16 W/m/K vs. 0.17 W/m/K).

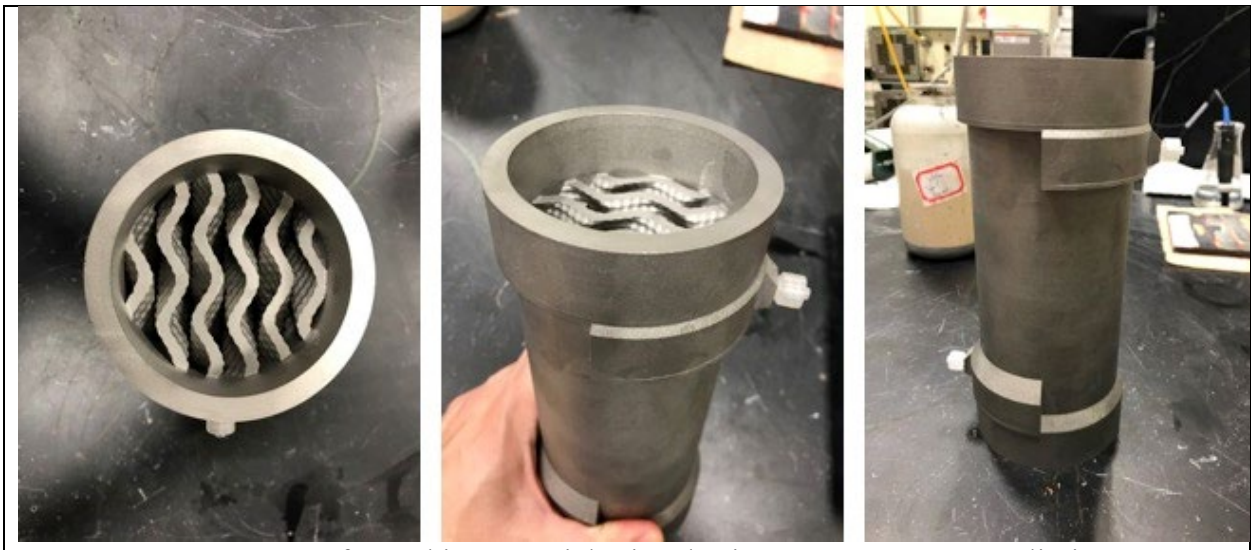

Exhibit 3.2.4. Heat transfer packing material printed using DMLS process to eliminate porosity during the printing process and provide high thermally conductive heat transfer surfaces.

4 EVALUATION OF PACKINGS ON 3" CO_2 CAPTURE BENCH UNIT

UK CAER's intensified technique was first evaluated on the 3" CO_2 capture bench unit using simulated flue gas to initially evaluate performance of the heat transfer packing and rich solvent dewatering membranes after which needed improvements were implemented for subsequent tests with coal-derived flue gas on the larger 0.1 MWth bench unit. Baseline tests on the 3" bench unit were first conducted without heat transfer packing material or membrane for reference comparisons and assessment of the individual components and the process as a whole.

4.1 Baseline Tests

The 3" bench unit consists of a 3" internal diameter clear PVC absorber column with 6ft 250Y stainless steel packing height, a 3" stripper column also with 4ft 250Y stainless steel packing height, an overhead condenser at the stripper exhaust for solvent recovery, a lean-rich heat exchanger and a hot-oil system that provides heat for solvent regeneration. The absorber and stripper are fitted with thermocouples for measuring the temperature profile in the columns. The unit is controlled with various instruments that measure solvent flow rates, temperatures and pressures. Two mass flow controllers (MFC) are used to control the flow rates of CO_2 and N_2, and the mixed simulated flue gas is sent to a saturator before being fed to the bottom of the absorber. A Horiba CO_2 analyzer is used to measure the concentration of CO_2 before and after absorber.

Experiments were done at given gas flowrate and liquid circulation rates to obtain baseline temperature profiles with only one type of stainless steel packing in the absorber. Similar experiments were also carried out at similar conditions by replacing portion of stainless steel with the insertion of two ABS 250Y sections with 1 ft total height with similar dimensions and features in the column. Representative conditions for the baseline tests and performance with CAER solvent is shown below in **Exhibit 4.1.1.** There was minimal variation in the capture efficiency of

~55% for the different conditions. Repeatable temperature profiles were obtained with five measurement points in the column as shown in **Exhibit 4.1.2** with the peak temperature typically occurring near TC2 and TC3, the second and third thermocouples respectively. Therefore, the location of the heat transfer packing material was chosen to be located between these two thermocouples, highlighted in green on the left in **Exhibit 4.1.2**, closer to the top of the column. After the stainless steel packing runs, the two packing sections between TC2 and TC3 were replaced with ABS packing modeled after 250Y. Similar performance and temperature profile were obtained as shown in **Exhibit 4.1.1** and **Exhibit 4.1.2** with this replacement.

Exhibit 4.1.1. Operating Conditions for Baseline Runs.

Date	Packing Material	Packing Orientation	Amine Flow Rate (mL/min)	Gas Flow Rate (L/min)	L/G	AB.TC.0 (°C)	Capture Efficiency (%)
3/29/19	SS	90°	453.1	128.65	2.83	45.2	55
4/2/19	SS	90°	451.5	128.67	2.82	45.5	55
4/4/19	SS	90°	452.9	128.06	2.84	46.1	55
4/9/19	SS	90°	452.3	130.47	2.78	44.5	55
4/10/19	SS	90°	449.2	130.31	2.77	45.4	56
4/18/19	ABS	90°	448.8	127.71	2.82	45.1	53

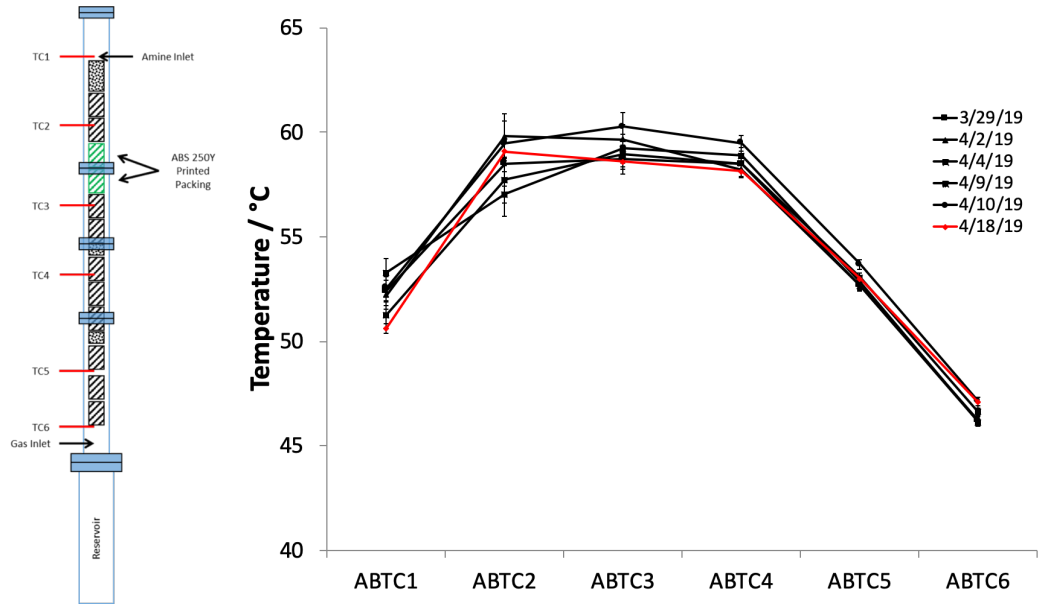

Exhibit 4.1.2. (Left) Locations for modifications to the packing material with 2 sections of ABS modeled after 250Y. (Right) Temperature profiles with (red) and without (black) ABS 250Y packing material.

4.2 Heat Transfer Packing Tests

On completion of the baseline runs, the absorber column was modified to incorporate heat transfer packings. Tests were performed with 3D printed ABS heat transfer packing material printed using FDM by 3D Hubs and also with the 3D printed stainless steel packing made using DMLS. The temperature profile from the baseline run with the 3D printed ABS heat transfer packing is shown in **Exhibit 4.2.1** along with a temperature profile after cooling water was circulated through the packing material. The cooling water temperature was set to 10 °C at a flow rate of 500 ml/min. At both TC2 and TC3, a temperature decrease of >14 °C was shown.

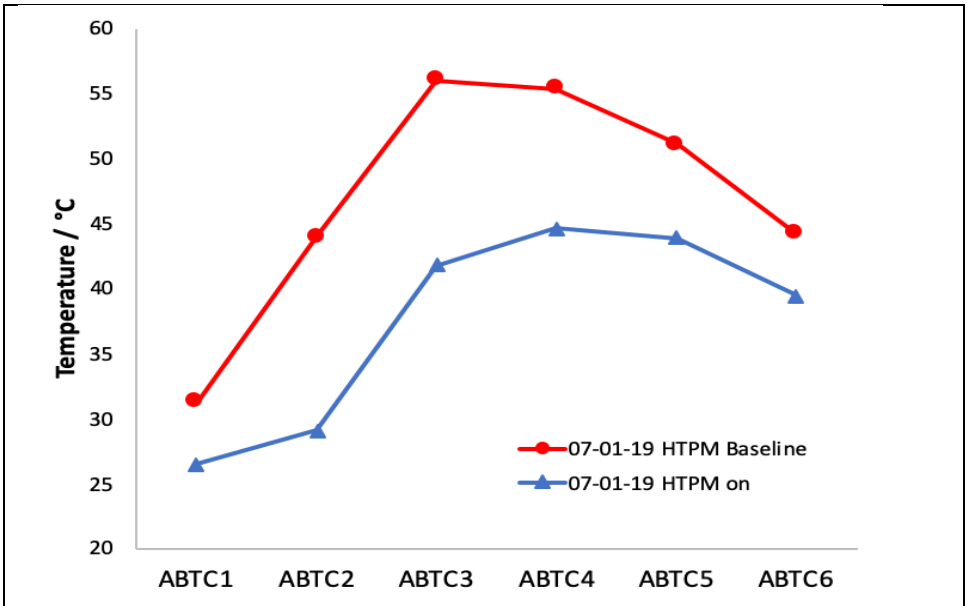

Exhibit 4.2.1. Temperature profiles with ABS heat transfer packing material (HTPM) as a baseline with no cooling water flow (red) and with 500 ml/min of 10 °C cooling water flow (blue).

The stainless steel heat transfer packing was also installed in the absorber between TC2 and TC3 where the peak temperature is located. **Exhibit 4.2.2** shows the location of the stainless steel heat transfer packing installation. This was operated with cooling water at a flow rate of 500 ml/min going through both sections of the packing and varied between 20-40 °C. The temperature profiles are shown in **Exhibit 4.2.3** for the inlet fluid to the column (TC0) as well as the six temperature measurements inside of the absorber (TC1-TC6). A baseline run is provided (black line) along with cooling water temperatures of 40 °C (blue dots) and 20 °C (red dashes). The test conditions for the polymer-based ABS heat transfer packings (top 4 rows) as well as the stainless steel heat transfer packing (bottom 3 rows) are shown in **Exhibit 4.2.4.**

As shown, the heat transfer packing could be used to successfully lower the peak temperatures with the flow of cooling water for heat recovery. The results from these tests informed operating conditions for the larger scale test on the 0.1 MWth bench unit. Future designs of the heat transfer packing sought to increase the void space from ~68% to ~97%, the void space for conventional 250Y packing. A balance between the cooling water inlet temperature/flow, gas velocity, and lean loading needed to be considered for increased capture rates.

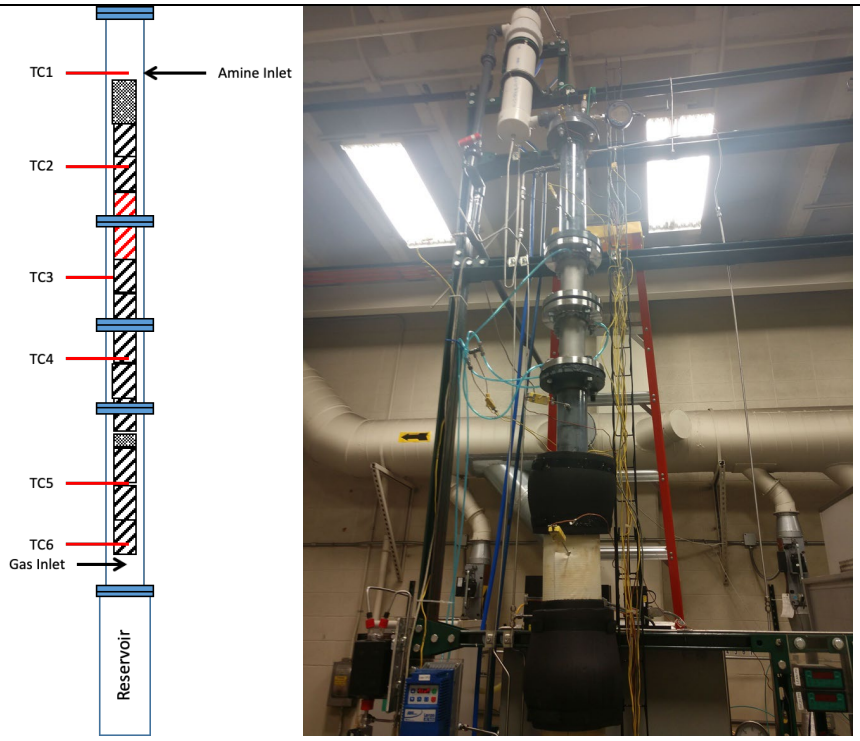

Exhibit 4.2.2. (Left) Locations where heat transfer packing was placed in the absorber column. (Right) Image of DMLS heat transfer packing installed in two sections of the absorber in the 3" bench unit with stainless steel flanges welded into place.

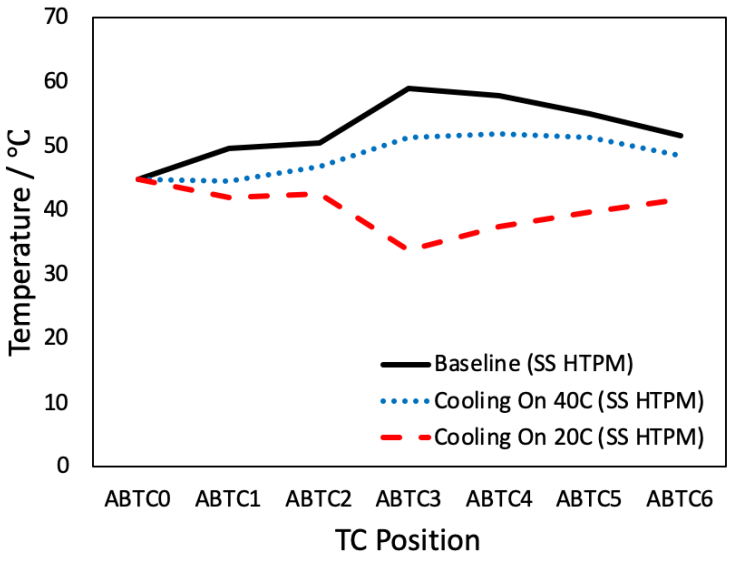

Exhibit 4.2.3. Temperature profiles with the DMLS heat transfer packing including a baseline run with no cooling water flow (black), with 500 ml/min of 20 °C cooling water flow (red), and with 500 ml/min of 40 °C cooling water flow (blue).

Exhibit 4.2.4. Example CO_2 capture data for heat transfer packings from the 3" bench unit using cooling water temperatures between 20-40 °C.

Packing & Cooling	Inlet Gas Velocity (m/s) & Temperature (°C)	Solvent Flow (ml/min)	% Capture	Lean Loading (mol/kg)	Rich Loading (mol/kg)	Lean C/N	Rich C/N
ABS Baseline	0.45 40.3	452.6	48.76	1.16	1.79	0.21	0.33
ABS Cooling20	0.45 40.4	452.5	44.45	1.1	1.65	0.21	0.33
ABS Cooling30	0.46 39.7	452.1	46.91	1.29	1.89	0.23	0.35
ABS Cooling40	0.46 40.2	450.9	46.83	1.16	1.79	0.21	0.35
S. Steel Cooling20	0.45 40.4	452.1	43.01	1.12	1.59	0.21	0.31
S. Steel Cooling40	0.45 40.1	451.5	48.63	1.27	1.85	0.22	0.34
S. Steel Baseline	0.45 40.2	450.6	49.26	1.4	1.97	0.24	0.37

5 ZEOLITE DEWATERING MEMBRANE MODULE DEVELOPMENT

The zeolite dewatering membrane dewaters the carbon-rich solvent ensuring a more concentrated solvent is sent to the stripper for regeneration. By dewatering, an increase of up to ~15% in the CO_2 partial pressure can be achieved resulting in significant reduction in the energy required per mole of CO_2 stripped. Leveraging CAER's previous work with zeolite-based membranes to dewater carbon-rich amine solvents, work focused on developing stable materials with desired fluxes, rejection rates, packing densities and alternative support materials to achieve this goal. Candidate materials were developed for initial testing on the 3" bench unit and subsequent scaling and testing on the 0.1 MWth bench unit. To overcome the barrier of scaling up the membrane module for testing at the 0.1 MWth bench unit, UK CAER collaborated with MPT at various developmental stages to facilitate the commercial production of the zeolite dewatering membrane with the desired packing densities and flux.

5.1 Membrane Synthesis Optimization

UK CAER has previously synthesized zeolite Y membranes with fluxes of ~3-5 kg m^{-2} h^{-1} for rich amine dewatering. Higher fluxes can, however, be achieved through the minimization of active layer thickness; which involve the use of smaller seed particles and shorter deposition times or

alternative support materials. Zeolite seed particles were therefore first synthesized and characterized using scanning electron microscopy (SEM) and x-ray diffraction (XRD). The zeolite seed particles are used to seed a ceramic support material (mullite or alumina) before a dense zeolite membrane layer is grown on the surface using a hydrothermal gel and elevated temperature. **Exhibit 5.1.1(a, b)** are SEM images of the as-synthesized zeolite seed particles. Particle sizes ranged from approximately 1.2-2.2 μm with an average particle size of <2 μm. Shown in **Exhibit 5.1.1c** are particles resulting from heating of the hydrothermal synthesis gel at 90 °C.

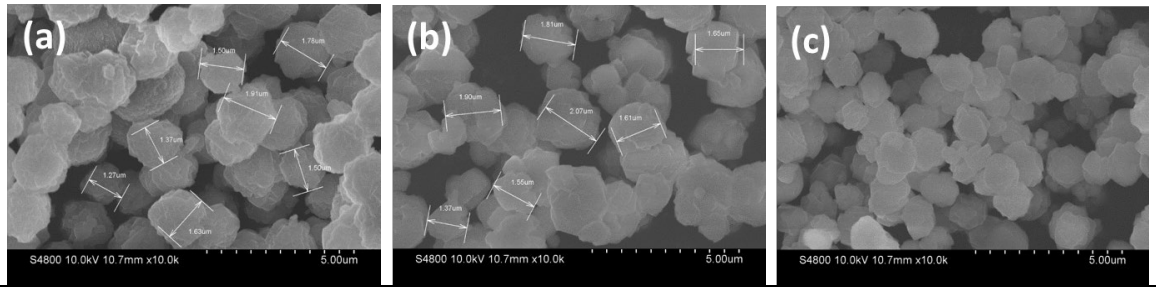

Exhibit 5.1.1. SEM images of (a) seed particles heated at 80 °C, (b) 100 °C, and (c) hydrothermal gel particles heated at 90 °C.

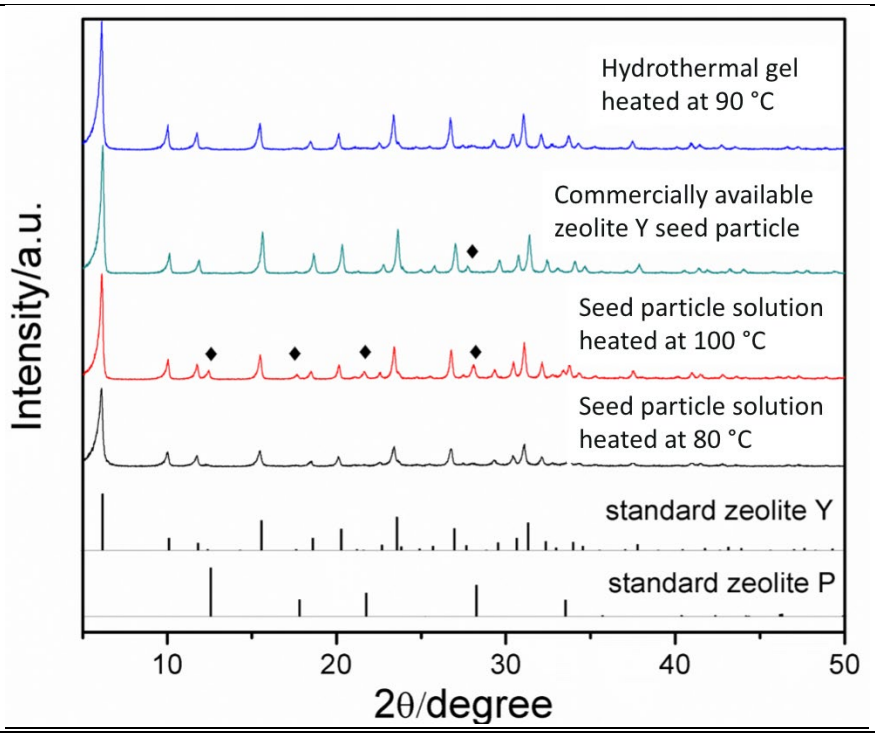

Exhibit 5.1.2. XRD of as-synthesized zeolite Y seed particles after heating at 80 and 100 °C as well as commercially available seed particles and confirmation of zeolite phase from heating hydrothermal gel at 90 °C.

XRD was used to confirm the zeolite phase present. Shown in **Exhibit 5.1.2** are the XRD patterns resulting from these particles as well as a commercially available zeolite Y seed particle and reference spectra for both zeolite Y and zeolite P. Both the seed particle solution heated at 80 °C and the hydrothermal gel heated at 90 °C only showed reference spectra for zeolite Y. However,

when the temperature was elevated to 100 °C, various reference peaks for zeolite P appeared. In addition, the commercially available zeolite Y seed particle contained one peak for zeolite P.
The synthesized seed particles were used to synthesize zeolite Y membranes on mullite (obtained from Ferroceramic) and alumina (obtained from MPT) support materials. The alumina support material from MPT was adopted as an option to decrease the cost and sourcing complexity of the scale-up process during module fabrication. Both alumina and mullite had been found to be chemically stable in the capture solvent and therefore the use of the alumina from MPT allowed for flexibility in the module design and attaining desired packing density due to the availability of multiple alumina diameters. Vacuum seeding and dip-coating were used as seeding methods of the synthesized particles on the MPT alumina support. Seeding conditions used were vacuum seeding: 3s, once; dip-coating: 5s, twice, upside down. **Exhibit 5.1.3** shows SEM images of the surface and cross sections of seed layer from dip-coating as well as vacuum seeding. Both vacuum seeding and dip-coating can yield a uniform seed layer for membrane growth on the MPT alumina support, although the density of the seed layer can change, as indicated by a slightly denser layer provided by the vacuum seeding process.

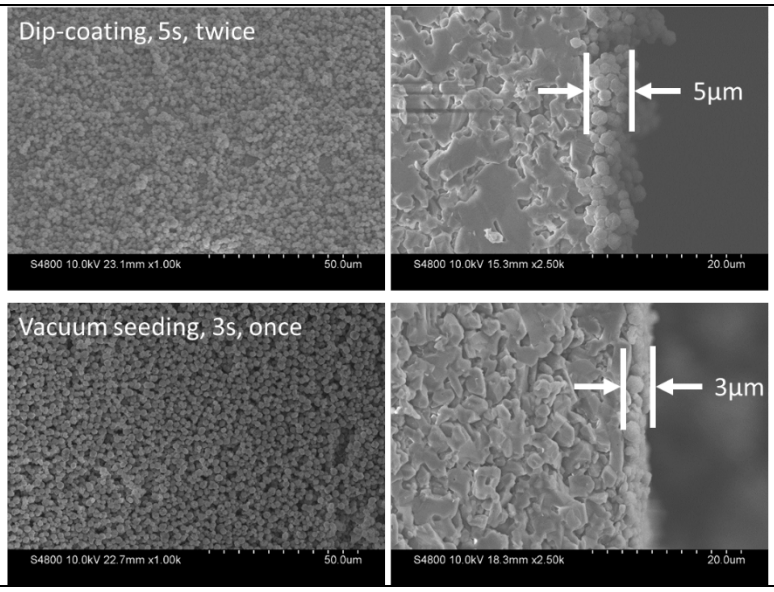

Exhibit 5.1.3. SEM images of NaY zeolite seed layers on MPT alumina support.

Zeolite membranes were subsequently synthesized following the dip-coating seeding method on three different alumina support diameters: S (5.7 mm), M (8.6 mm), and L (11.8 mm). The SEM images of the surface (1a, 2a, 3a) and cross sections of the sample showing the dense surface layer (1b, 2b, 3b) are shown in **Exhibit 5.1.4**. X-ray diffraction (XRD) was used to analyze the membrane surface and confirm the presence of the zeolite Y phase. XRD data is shown for these samples in **Exhibit 5.1.5** along with reference points for the alumina support, zeolite Y, and zeolite P.

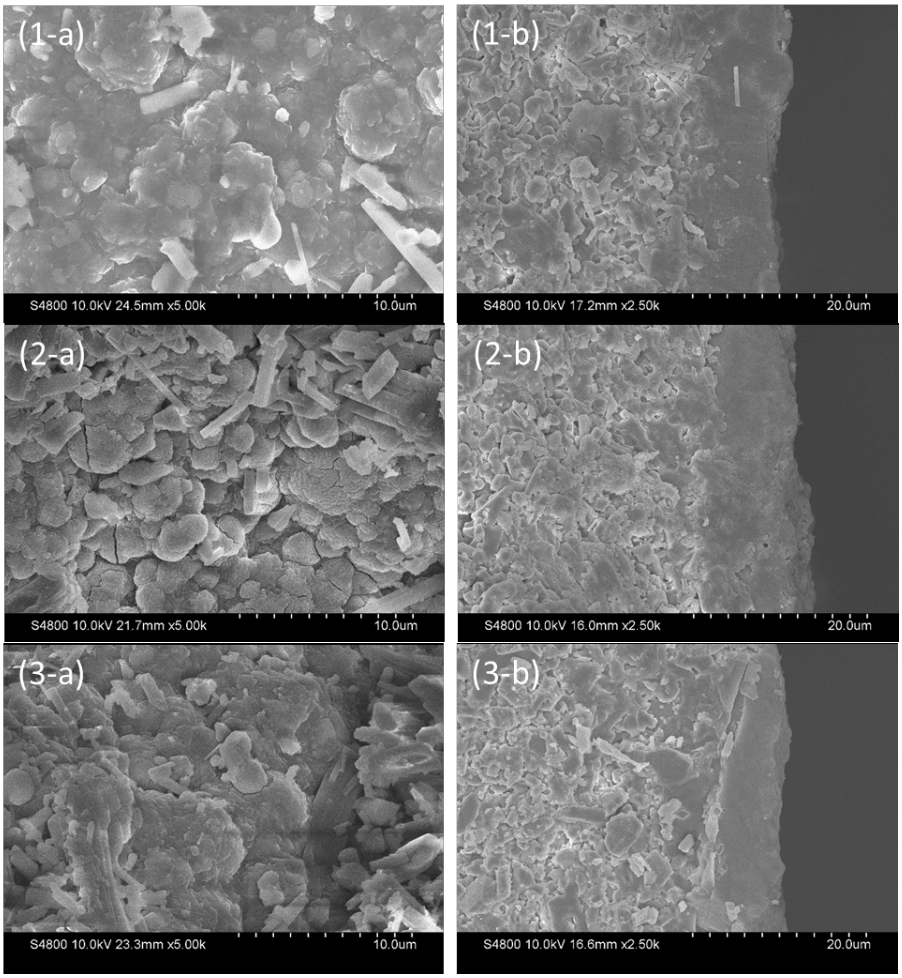

Exhibit 5.1.4. NaY zeolite membranes prepared on alumina substrates from Media & Process Technology: Sample (1-3), (a) Surface area and (b) Cross-section. Sample 1 is L, sample 2 is M, and sample 3 is S.

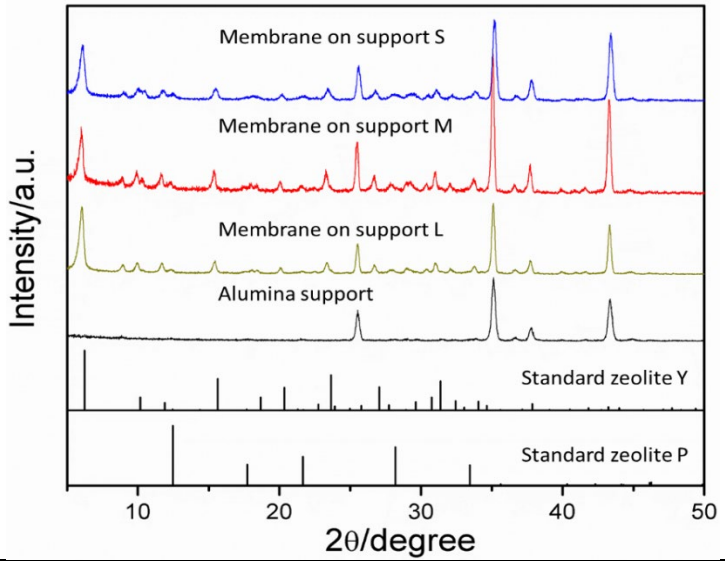

Exhibit 5.1.5. XRD patterns of NaY zeolite membranes prepared on MPT alumina substrates.

As part of the synthesis transfer process for membrane scale-up, which consisted of seed particle synthesis/deposition and a zeolite membrane hydrothermal growth step, UK CAER shared the seed particle synthesis process/procedure with MPT. In the collaboration, UK CAER adapted a QA/QC test from MPT in an effort to determine type and quantity of membrane defects during the synthesis. In this test, a zeolite membrane is immersed in an isopropanol (IPA) bath and a pressurized nitrogen supply is attached to one end of the membrane while the other end is sealed. Pressure is increased on the sample up to 30 psi. If gas bubbles are found at <15 psi it would indicate that there is a lack of dense zeolite at that location. An example of a poor membrane layer is shown for comparison in **Exhibit 5.1.6a** while a complete membrane layer is found in **Exhibit 5.1.6b**. Membranes were checked using this test to minimize any large batch synthesis difficulties.

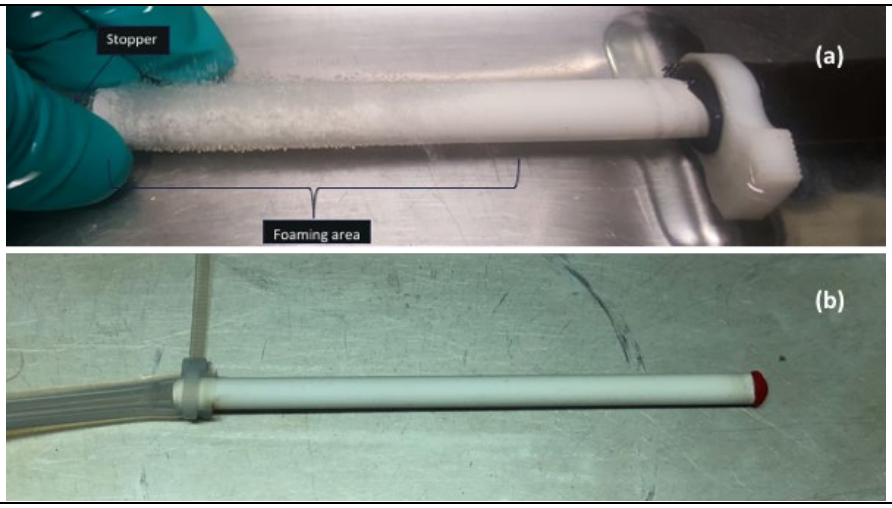

Exhibit 5.1.6. Images from QA/QC testing for (a) incomplete membrane surface layer and (b) full membrane coating on alumina support.

5.1.1 Synthesis Modifications and Dewatering Tests

Modified Supports

Dense zeolite layers could be synthesized on surface of the MPT alumina support with a pore size of 0.5 µm, but infiltration of precipitates was evident in the support and this effectively increased the membrane thickness but decreased the flux. Zeolite Y membranes were then synthesized on a modified alumina support provided by MPT. The new 0.05 µm pore size alumina support had a dense alumina layer of approximately 30 µm in thickness on top of the standard alumina support. This dense layer had an average pore size of only 0.05 µm while the standard support had an average pore size of 0.5 µm. With the modified, denser alumina layer, the zeolite layer and any resulting precipitates from the hydrothermal growth phase are kept further confined to the surface (shell-side) of the alumina. SEM images of the surface and cross-section of this new membrane are shown in **Exhibit 5.1.7**. Crystal growth of the resulting zeolite is evident from both the cross-sectional SEM as well as the surface image. These membranes were seeded using a dopamine deposition process for 20 h followed by hydrothermal growth at 85 °C for 11 h.

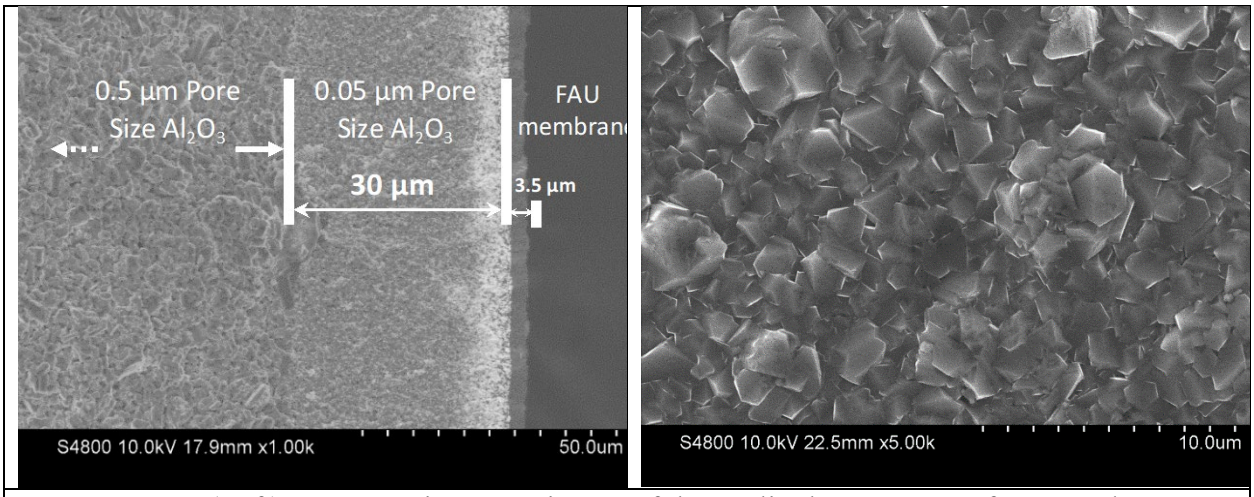

Exhibit 5.1.7. (Left) Cross-section SEM image of the zeolite layer on top of 0.5 µm dense alumina support from MPT, (Right) Zeolite Y surface layer showing crystal formation for membrane grown on alumina support with pore size of 0.05 µm from MPT using 85 °C and 11 h during hydrothermal growth.

Dewatering Tests in Amine

Dewatering tests of multiple membranes with different support tube types were done using an amine solvent at 130 °C and 75 psi. The fluxes and rejection rates are highlighted in **Exhibit 5.1.8**. The membranes grown at 85 °C for 11 h demonstrated repeatable high performance with both support materials, mullite and alumina, demonstrating flux values >5 kg m^{-2} h^{-1} and rejection rates of >90% when assessed by the rejection of carbon loaded amine solvent. When the hydrothermal growth time was limited to just 10 h, flux was retained but there was a significant drop in the rejection rate. While this may be due to limited membrane defects during this synthesis, the 11 h membranes appear to meet the process requirements. Zeolite membranes were also synthesized at a higher temperature; in this case 100 °C, using both 0.05 µm and 0.5 µm pore size alumina support materials. A shorter hydrothermal growth time of 4 hours was used here due to the increase in crystal growth kinetics and precipitation from the gel solution at this elevated temperature. A reasonably high flux of >4 kg m^{-2} $h^{-1}$was achieved along with a rejection rate of >80% for the zeolite membrane grown on the 0.05 µm pore size alumina. However, much lower flux and rejection were achieved for the 0.5 µm pore size alumina support. Confining of the zeolite layer to just the surface of the support was crucial for the chosen synthesis process.

Exhibit 5.1.8. Fluxes and rejection rates for zeolite membranes in amine solvent.

Support	Synthesis Temperature (°C)	Hydrothermal Time (h)	Flux (kg m^{-2} h^{-1})	Rejection Rate (C Loading) (%)	Rejection Rate (Total Alkalinity) – (%)
0.05 µm MPT-S	85	11	6.58	94.37	>99
0.05 µm MPT-S	85	11	5.11	91.40	85.78
0.05 µm MPT-S	85	10	6.12	62.07	55.47
0.05 µm MPT-S	100	4	4.32	82.72	93.43
0.5 µm MPT-S	100	4	1.89	30.44	20.10

* MPT-S designates the small diameter alumina support from MPT (5.7 mm OD).

Seeding Process Modification

In order to increase the flux through the membrane layer, a shorter polydopamine seeding period was used as longer seeding times could potentially result in more particle deposition in the alumina support increasing the resistance to water transport. Dopamine deposition times of 4, 8, 15 and 20 hr on the 0.05 µm alumina support were investigated. The zeolite membrane growth was done at 85 °C and 11 h hydrothermal growth. As shown in the SEM images in **Exhibit 5.1.9** for the different seeding times, the surface morphologies of the membranes remained intact with plate-like structure indicative of the formation of zeolite Y crystals. As desired, the membrane thickness decreased from ~3.5 µm for 20 hours of dopamine deposition to 2 µm for 4 hours of deposition.

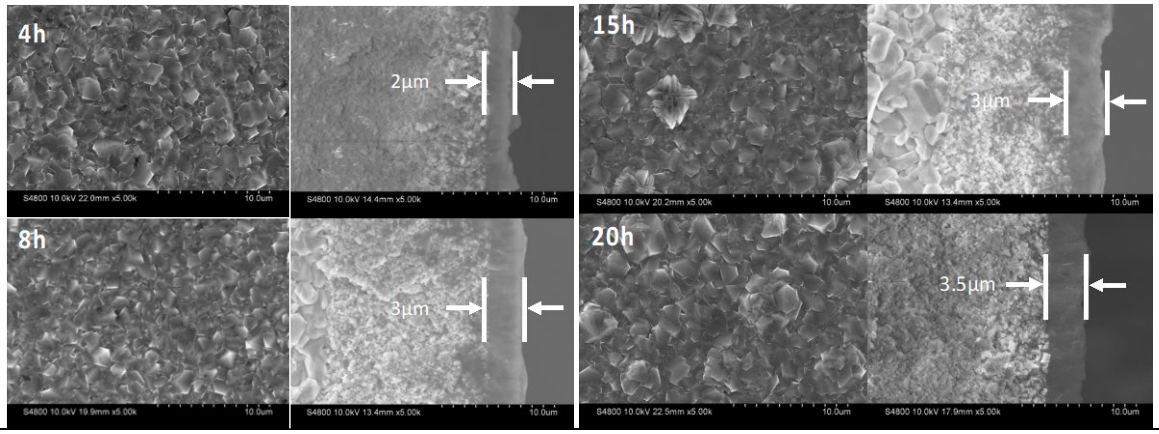

Exhibit 5.1.9. SEM images of the zeolite layer on top of dense alumina support from MPT using dopamine deposition times of 4, 8, 15, and 20 hours. For each membrane, surface (left) and cross-section (right).

Dewatering Tests in Amine/Amine Blends

Exhibit 5.1.10. Fluxes and rejection rates in MEA for zeolite membranes.

Dopamine Modification (h)	Flux (kg m^{-2} h^{-1})	Rejection Rate (C Loading) (%)	Rejection Rate (Total Alkalinity) (%)
4*	8.36	>69	>65
4	4.21	91.67	88.65
8	1.77	85.83	87.66
15	2.20	84.78	86.18
20	3.58	>90	>90

*Run at 148 °C and 150 psi in MEA. All others at 135 °C and 75 psi.

From the results for dewatering tests carried out in monoethanolamine (MEA) solvent mostly at 135 °C and 75 psi shown in **Exhibit 5.1.10**, the highest flux was seen with the 4 h dopamine deposition, reaching over 8 kg m^{-2} h^{-1} when operating at an elevated temperature. However, there does not appear to be a distinct trend in the flux. Shorter deposition times did not completely correlate to higher fluxes, even though the highest values are seen for 4 hours of deposition. Since blended solvents, such as the CAER solvent, are routinely used in CO_2 capture with distinct

physical properties, the dewatering tests were also done in a blended amine. The results for a typical 4 h dopamine modified zeolite Y membrane dewatered at 130 °C at a transmembrane pressure of 75 psi in a blended amine is shown in **Exhibit 5.1.11.** The flux of the membrane started at ~2 kg m^{-2} h^{-1} and increased to ~3.5 kg m^{-2} h^{-1} during the 5.5 hour test. The rejection rate was maintained at >90% in the first 3.5 h after which it gradually declined.

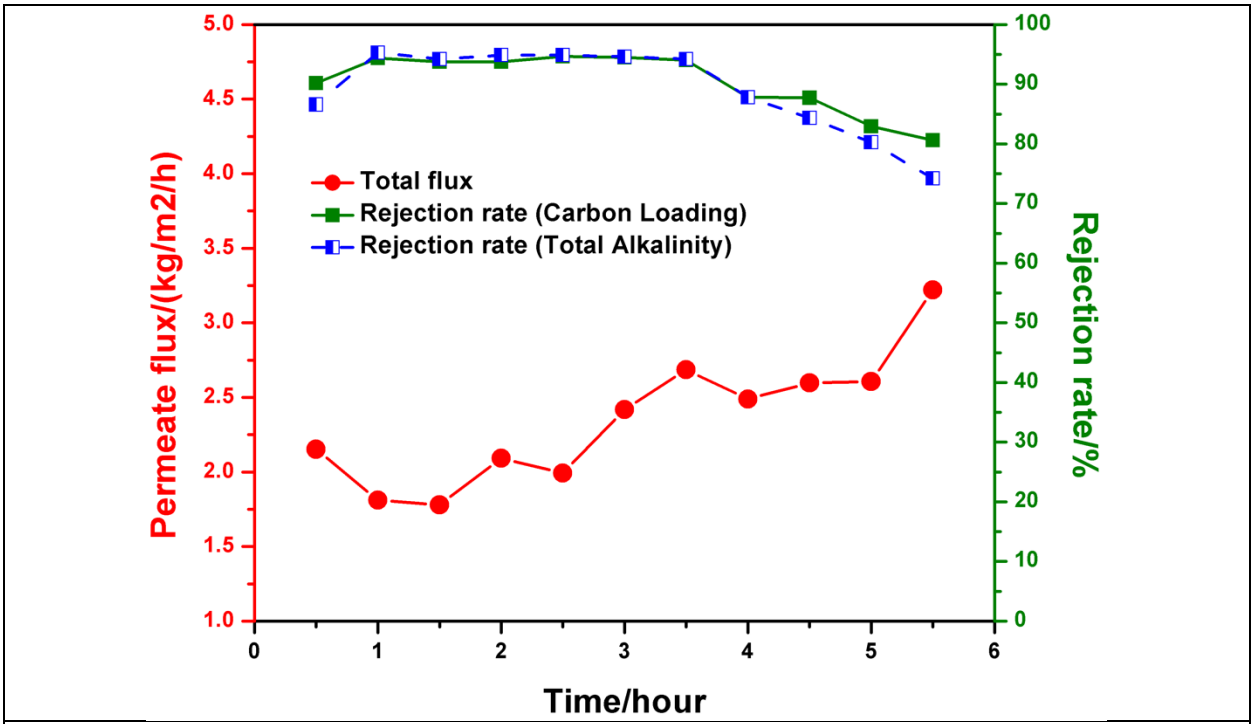

Exhibit 5.1.11. Flux and rejection rate for zeolite Y membrane grown on a 0.05 µm pore size MPT alumina support using a dopamine deposition time of 4 hours dewatered at 130 °C and 75 psi in a blended amine solvent.

The loss of rejection rate over time is indicative of membrane instability, which may be due to hydrolysis of silanol sites at higher water content and elevated temperature. The use of 130 °C will exacerbate this issue. Therefore, follow-up testing focused on a lower amine solvent temperature of 120 °C but still using a transmembrane pressure of 75 psi with results shown in **Exhibit 5.1.12.** The rejection rate held at >90% for over 8 hours, showing an improvement to the dewatering experiments carried out at 130 °C. However, the flux decreased as anticipated due to the lower temperature of the feed solution and lower transmembrane water driving force.

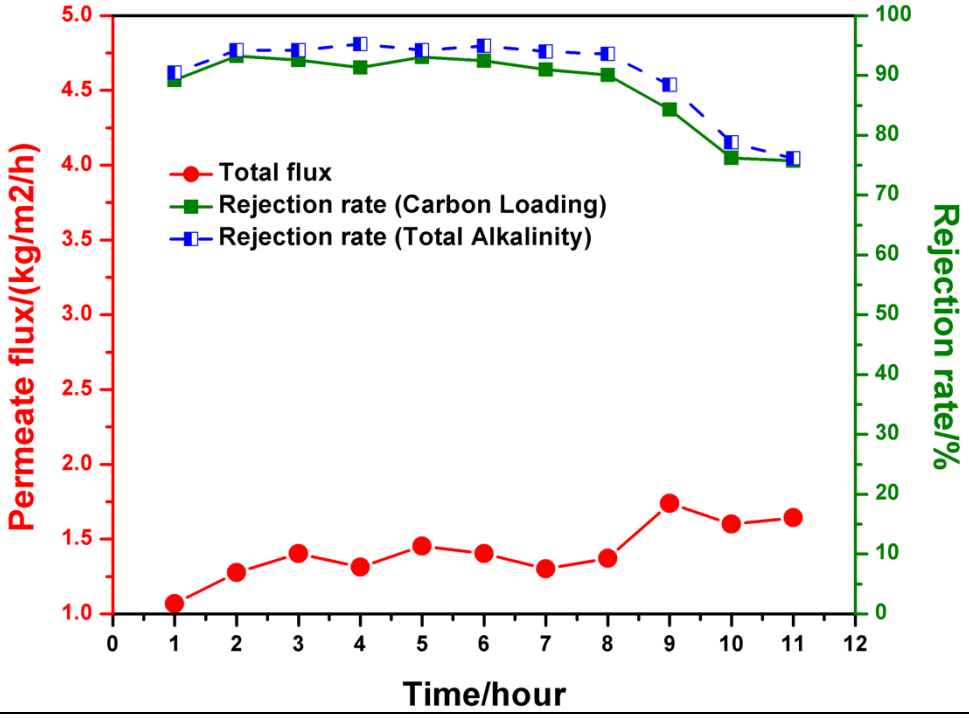

Exhibit 5.1.12. Flux and rejection rate data for zeolite Y membrane grown on a 0.05 µm pore size MPT alumina support using a dopamine deposition time of 4 hours dewatered at 120 °C and 75 psi in a blended amine solvent.

5.1.2 Zeolite Y Membrane Stability

To evaluate the suitability of the zeolites for prolonged operation in the capture process, stability tests were performed on the synthesized membranes. The test was done with a zeolite Y membrane grown on a 0.05 µm pore size MPT alumina support using a dopamine deposition time of 4 hours and their stability compared to commercial zeolite Y particles from Zeolyst in carbon loaded CAER solvent. In both the zeolite membrane and Zeolyst stability tests, 90 mL CAER solvent was placed into a Teflon vessel and heated up to 80-120 °C for 120 hours. In the first control test with Zeolyst, 1 g of Zeolyst CBV100 particles was used, and SEM and XRD analyses were gathered before and after stability testing at 120 °C for 120 hours. Shown in **Exhibit 5.1.13** are XRD patterns and SEM images of the Zeolyst particles before and after immersion in solvent at 120 °C for 120 hours. No significant difference is seen in either the XRD patterns or the SEM images, indicating that the zeolite is stable under these conditions including elevated temperature and carbon loading. However, from the SEM images of the zeolite Y membrane shown in **Exhibit 5.1.14,** changes to the membrane surface can be seen starting at 110 °C, which is shown in the intercrystal area. Therefore, while the Zeolyst particle is stable, the operating temperature for the zeolite membranes grown on the MPT alumina support should be maintained between 100-110 °C. This necessitated the quest for alternative support materials to improve the membrane stability at relative higher temperatures and also to increase the flux through the zeolite membranes as the support can play a critical role involving membrane adhesion and also water transport.

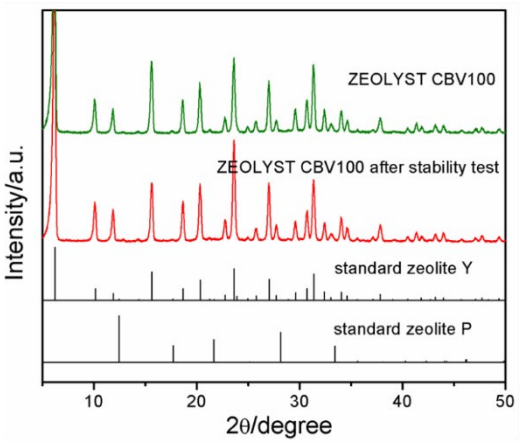

Exhibit 5.1.13. XRD patterns and SEM pictures of ZEOLYST CBV100 particles before/after stability test.

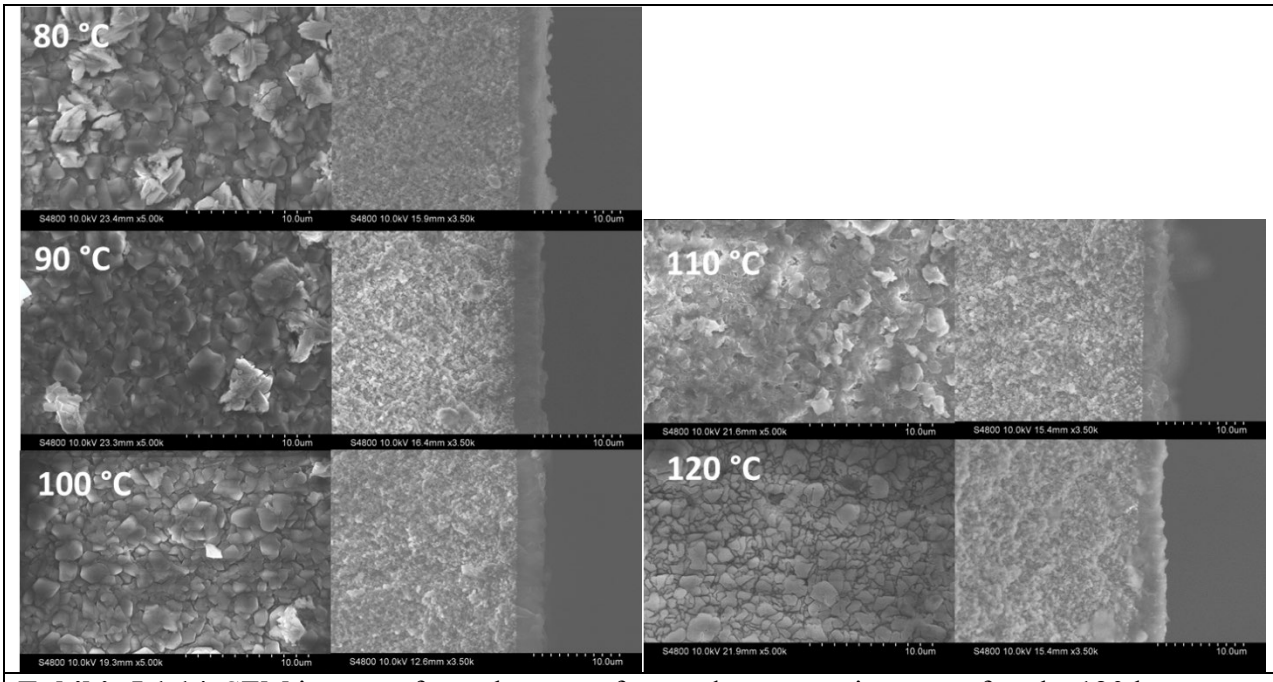

Exhibit 5.1.14. SEM images of membrane surface and cross-section area after the 120 hour stability test at temperatures from 80-120 °C.

5.1.3 Alternative Membranes

With concerns about the stability of the membranes on the MPT support at operating conditions in the capture process, more stable alternatives were also explored. Some of these included using (i) alumina support from Nanjing Tech., and (ii) mullite support from Nikata.

A support from NanjingTech, AC100, an alternative alumina support with an O.D. of 12 mm and

~0.1 μm pore size was tested. This support is similar to the one from MPT with a ~28 μm dense Al_2O_3 layer on the surface and pore size of 0.1 μm. Testing using this AC100 support was conducted at temperatures of up to 140 °C, higher than used in the previous stability test, to examine separation performance under more extreme conditions. Using a 30 wt% MEA solution, 140°C, 100 psi, and 30 mL/min yielded a flux of up to 10.12 kg m^{-2} h^{-1}. An initial rejection rate of 88.3% was achieved, demonstrating that changes in the support material can also impact the resulting flux. Membranes were also synthesized on a Nikkato mullite support. The resulting membrane thickness was approximately 5.5 μm and was composed of both sodium Y (NaY) and sodium P (NaP) zeolite phases. The rejection rates from this membrane were low due to the lack of a consistent and uniform membrane on the surface of the mullite. A conventional seeding process, as opposed to a dopamine seeding method, may be more conducive to generate a membrane layer on the surface due to the lack of a dense support layer to confine the zeolite layer.

Based on the higher performance achieved with the alumina support from Nanjing Tech, adaptations had to be made to MPT dense layer alumina supports for the large-scale membrane module synthesis to improve performance.

Zeolite membrane synthesis using APTES ((3-aminopropyl)triethoxysilane) modified substrate

A seeding-free method for zeolite membrane preparation with APTES (3-aminopropyl triethoxysilane) modified substrate was used to form thinner membrane layer. APTES functions as covalent linker and part of Si source during the formation of membrane thin layer (Zhou et al, 2020). APTES modified substrates were prepared with 0.005, 0.05, 0.5 wt% in toluene for 0.5 and 1 hr and the membranes were synthesized at 75 °C for 24 hr and 85 °C for 16 hr. As shown in **Exhibit 5.1.15** from bubble tests, membranes prepared on substrates modified in 0.05, 0.5 wt% APTES/toluene have less defects. Dewatering performance of select membranes were carried out in CO_2 loaded 30 wt% MEA solution and IPA/H_2O solution. In MEA, a membrane flux of 3.8 kg/m^2/hr and 98% rejection rate was obtained and a 3.6 kg/m^2/hr membrane flux, 98% rejection rate was also obtained with IPA/H_2O (**Exhibit 5.1.16)**. However, after testing in IPA/H_2O at 110 °C for 2 days, the rejection rate dropped to below 80%.

Exhibit 5.1.15. Membranes prepared by different conditions of seeding-free method and the bubble test results.

Membrane ID	**APTES/Toluene: Concentration, treatment temperature & duration**	**Membrane synthesis conditions**	**Bubble test (IPA) at 30 psi of N_2**
NaY-AP01	0.005%, 110°C/1hr	75°C/24hr	Top section foamed. Bottom section had less than 10 streamers.
NaY-AP02	0.005%, 110°C/1hr	85°C/16hr	4.5 in top section foamed.
NaY-AP03	0.05%, 110°C/30min	75°C/24hr	2 bubble-line streamers.
NaY-AP04	0.05%, 110°C/30min	85°C/16hr	1 thin streamer.
NaY-AP05	0.5%, 110°C/30min	75°C/24hr	1 thin streamer near the opening.
NaY-AP06	0.5%, 110°C/30min	85°C/16hr	Two streamers. One on each end.

Exhibit 5.1.16. Dewatering performance of membranes prepared on APTES modified substrates.				
Zeolite Membrane ID	**Dewatering test in CO_2 loaded 30 wt% MEA**			
	Temperature (°C)	**Pressure (psig)**	**Total Flux (kg m^{-2} h^{-1})**	**Rejection Rate (%)**
NaY-AP04	106	78	0.5	98
	116	78	1.4	98
	126	78	3.3	98
	131	78	3.8	98
NaY-AP03	**Dewatering test in 70 wt% IPA/water**			
	110	Vacuum on permeate side	3.6	98

Membrane protection layer by 3-aminopropyltriethoxysilane (APTES) grafting

In an alternate membrane synthesis, APTES was grafted on the membrane as a protection layer. The as-synthesized NaY membranes (NaY-6.29) by seeding-hydrothermal growth method were grafted with APTES solution (1mM in 50 mL toluene) in rotating autoclaves at 110 °C for 1 h. The APTES-grafted NaY membranes were further washed thoroughly with ethanol and dried at 120 °C overnight under nitrogen atmosphere. **Exhibit 5.1.17** shows the membrane morphology change. In **Exhibit 5.1.17**, a-b are the as-synthesized membrane, c-d are NaY membrane surface after grafting with APTES, e-f are membrane surface after stability test in CAER solvent. According to the literature, the modification layer thickness should be ~ 500 nm, however, not distinct on the NaY membrane. This modified membrane was tested for stability in 30 wt% MEA at 137 °C and CAER solvent at 110 °C. In 30 wt% MEA, the rejection rate of APTES-NaY membrane dropped to <50% after 4 h (**Exhibit 5.1.18**), however, only 8 streamers were found in the IPA bubble test. In CAER solvent, the membrane was found to be leaking after 20 h.

The grafting procedure was similarly applied to the NaY membrane (MPT-NaY-51B) provided by MPT which was grafted with APTES solution (1 mM in 50 mL toluene) in rotating autoclaves at 110 °C for 1 h. The APTES-grafted NaY membranes were further washed thoroughly with ethanol and dried at 120 °C overnight under nitrogen atmosphere. This modified membrane was also tested for stability in CAER solvent at 110 °C, 75 psig. The membrane flux decreased from 0.03 to 0.004 kg m^{-2} h^{-1}. Rejection rate started to show a decreasing trend after testing for 95 hr. To better understand the dewatering performance, EDX was used to determine the membrane composition after the dewatering test in CO_2-loaded CAER solvent. The Si/Al ratio dropped from 1.1 to 0.7 on the membrane without APTES modification. The loss of Si was mitigated on the APTES-modified membranes, which could be the main reason for membrane degradation. The results for the stability tests and membrane composition after dewatering tests are shown in **Exhibits 5.1.19** and **5.1.20** respectively.

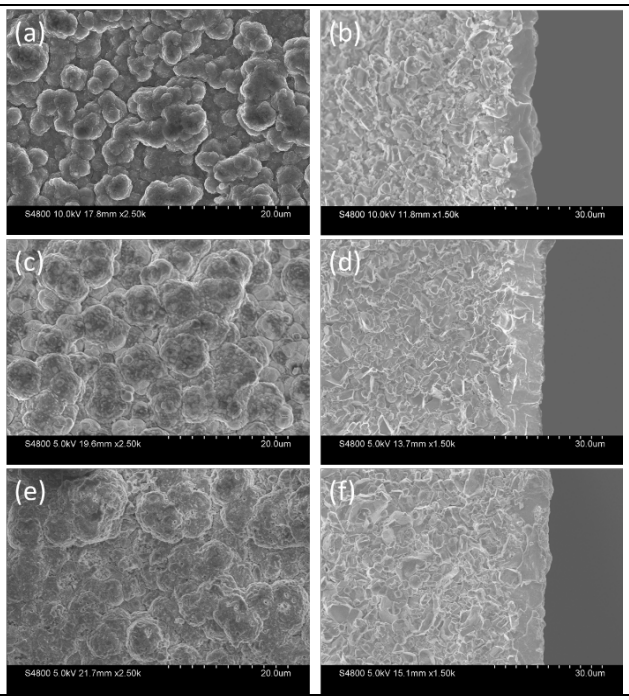

Exhibit 5.1.17. Membrane morphology (a, b) as-synthesized NaY membrane; (c, d) after APTES grafting for 1 h; (e, f) after stability test in CAER solvent at 110 °C for 20 h.

Exhibit 5.1.18. Dewatering test of APTES-grafted membranes in different amine solutions.

Dewatering test solution	Dewatering Test Conditions					IPA bubble test
	Temperature (°C)	Pressure (psig)	Testing time (h)	Total Flux (kg m^{-2} h^{-1})	Rejection Rate	
30 wt% MEA	137	75	4	0.43	43.1%	8 streamers
CAER Solv.	110	75	20	leaking	8.2%	Foaming

Exhibit 5.1.19. Stability test of APTES-grafted MPT membranes in CO_2-loaded CAER solvent at 110 °C, 75 psig.

	Dewatering test solution	Dewatering Test Conditions				
		Temperature (°C)	Pressure (psig)	Testing time (h)	Total Flux (kg m^{-2} h^{-1})	Rejection Rate
APTES-MPT-NaY-51B	CAER solvent	110	75	24	0.003	94.0%
		110	75	48	0.004	93.5%
		110	75	72	0.004	88.3%
		110	75	95	0.004	74.0%

Exhibit 5.1.20. Membrane composition after dewatering test in CO_2-loaded CAER solvent at 110 °C, 75 psig.

Membrane	Si/Al atomic ratio					
	1	2	3	4	5	Average
NaY-6.29 before stability	1.09	1.08	1.18	1.25	1.06	1.13±0.08
NaY-6.29 after stability test	0.50	0.77	0.57	1.28	0.56	0.74±0.32
APTES-NaY-6.29 after stability test	0.97	0.89	0.59	1.21	0.90	0.91±0.22
MPT-NaY-51A after stability test	1.14	1.19	1.13	1.15	1.17	1.16±0.02
APTES-MPT-NaY-51B after stability test	1.23	1.18	1.29	1.18	1.22	1.22±0.08

5.2 Membrane Modules Assembly and Testing

Using the synthesis procedure described above in section 5.1.1 for zeolite Y membranes grown on dense alumina supports, MPT constructed membrane modules that were tested at UK CAER. The 10-inch long, 3-membrane bundles were tested in CAER solvent at 100 °C, 80 psi, and 30 mL/min. The flux and rejection rates for the 3-membrane bundle are shown in **Exhibit 5.2.1** along with single membrane tests for comparison. Although the rejection rates were high, higher fluxes were desired. Subsequently, MPT constructed a membrane module composed of 19 membranes with OD of 5.7 mm and length of 483 mm (19") to be tested in the 3" CO_2 capture bench unit. The total volume of the membrane module was 634 cm^3 with a total membrane area of 1642 cm^2 and a resultant packing density of 259 m^2/m^3. A picture of the membrane bundle is shown below in **Exhibit 5.2.2**. The end cap material is Garolite, which was tested at 120 °C for >100 hours and showed no changes.

Exhibit 5.2.1. Fluxes and rejection rates for MPT membranes in dewatering tests in CAER solvent.

Membrane	Temperature (°C)	Flux (kg m^{-2} h^{-1})	Rejection Rate (C Loading) (%)
1 membrane, 4 in	85	0.18	94.68
1 membrane, 4 in	110	0.84	90.37
3 membranes, 10 in	100	0.61	95.2

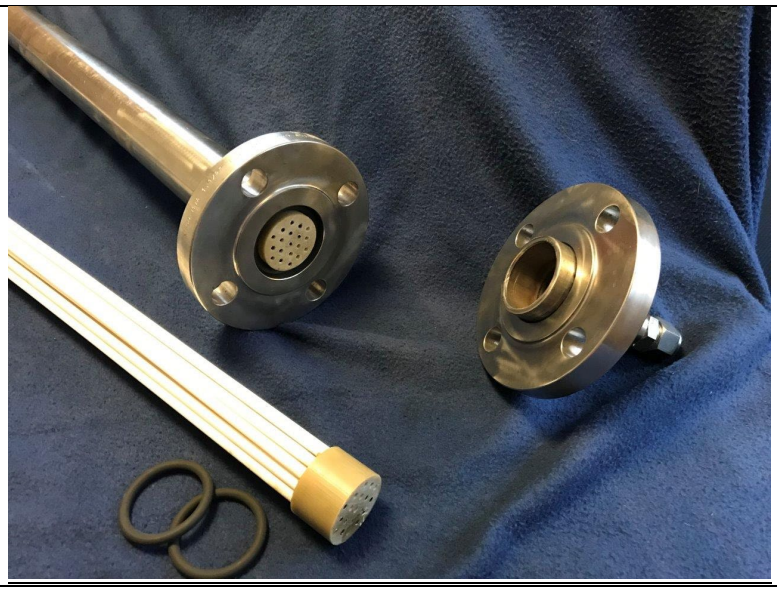

Exhibit 5.2.2.19 membrane module tested in the UK CAER 3" CO_2 capture bench unit. Packing density of >250 m^2/m^3 achieved with this bundle.

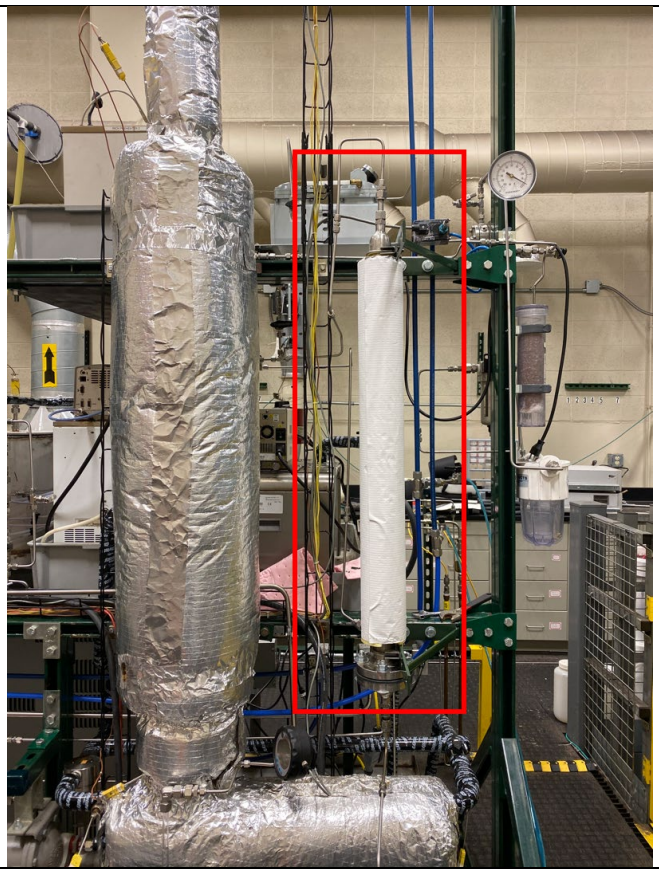

Exhibit 5.2.3. Installation of 19" zeolite membrane module from MPT (outlined in the red box) in 3" CO_2 capture bench unit.

The 19 membrane module was installed and tested in the 3" CO_2 capture bench unit as outlined in the red box in **Exhibit 5.2.3** with CAER solvent. Testing focused on flux and rejection rate determinations from the module as well as design considerations for scale-up to the 0.1 MWth bench unit. After fixing initial leak points in the module, experiments were performed over a number of days to assess membrane dewatering performance and stability. **Exhibit 5.2.4** shows the rejection rate and flux versus time. Samples #1 to #4 belong to Day 1 of testing. Sample #1 is the initial 30 min sample, which shows the highest rejection rate. Rejection rate was recovered to around 90% by sample #3. Back pressure was added into the test system starting from sample #4, and the flux kept increasing. Samples #5, 6, and 7 are for a continuous 6 hour test on days 2-4. The rejection rate derived from the total alkalinity, dropped for the first two data points each day due to system startup with a lean amine stream. After running for four days for a total of 22 hours, the membranes still showed a rejection rate higher than 80%. The test conditions are summarized in **Exhibit 5.2.5**. The sustained rejection rates were promising even though further work was still required to improve the flux through the membrane. The detected leak points and the approaches adopted to leak-proof the module together with the testing results provided focus areas for design improvements and suitable test conditions for the scaled-up module installation and testing in the 0.1 MWth bench unit.

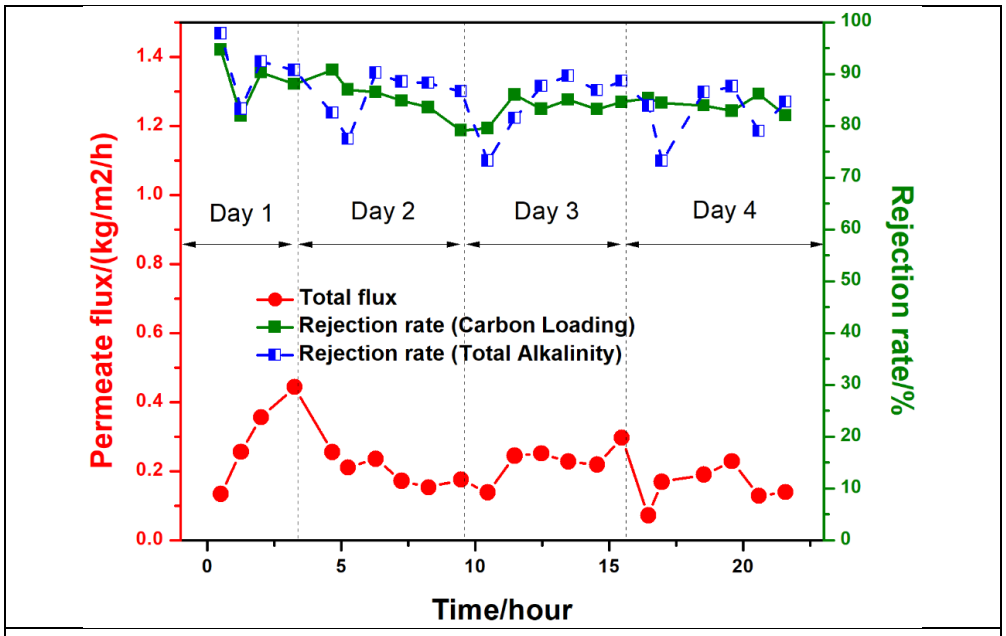

Exhibit 5.2.4. Rejection rate and flux versus time for 9-membrane bundle dewatering test in 3" CO_2 capture bench unit.

Exhibit 5.2.5. Test conditions and sample analysis for membrane evaluation in 3” bench unit.								
Sample	**Inlet/outlet Temp. (°C)**	**Pressure (psig)**	**Test time (min)**	**Vacuum degree (inHg)**	**Flow rate (ml/min)**	**Flux kg m^{-2} h^{-1}**	**Rejection rate (C loading)/ %**	**Rejection rate (total alkalinity)/%**
1	90/90	0	30	28	150	0.13	94.66	97.80
2	90/90	0	45	28	150	0.26	81.94	83.25
3	90/80	0	45	28	200	0.36	90.29	92.40
4	90/86	80	75	28	150	0.44	88.07	90.71
5-1	90/86	80	60	28	200	0.25	90.77	82.46
5-2	90/90	80	60	28	170	0.21	86.99	77.43
5-3	91/90	80	60	28	160	0.24	86.51	90.19
5-4	91/90	80	60	28	160	0.17	84.80	88.49
5-5	91/90	80	60	28	165	0.15	83.57	88.24
5-6	91/90	80	60	28	165	0.18	79.09	86.62
6-1	91/88	80	60	28	168	0.14	79.51	73.25
6-2	92/91	80	60	28	165	0.24	85.99	81.49
6-3	91/90	80	60	28	152	0.25	83.24	87.65
6-4	91/90	80	60	28	180	0.23	85.00	89.64
6-5	91/90	80	60	28	170	0.22	83.19	86.81
6-6	91/89	80	60	28	170	0.30	84.56	88.63
7-1	78/76	80	60	28	175	0.09	85.31	83.91
7-2	90/89	80	60	28	182	0.19	84.43	73.24
7-3	90/90	80	60	28	175	0.21	83.91	86.53
7-4	91/89	80	60	28	165	0.25	82.86	87.62
7-5	91/91	80	60	28	178	0.15	86.09	78.96
7-6	91/91	80	60	28	170	0.16	81.98	84.64

6 EVALUATION AT 0.1 MWth CO_2 CAPTURE BENCH UNIT

On completion of initial assessments of aspects of the process on the 3" unit, a full evaluation was carried out on the 0.1 MWth CO_2 capture bench unit with the implementation of identified improvements such as heat transfer packing and dewatering membrane designs and suitable operating conditions. The unit was retrofitted for the installation of the in-situ heat transfer packing in the absorber, a split flow to the stripper which required another entry port to the stripper with accompanying additional heat exchanger and flow modifications for the incorporation of the dewatering membrane module. Tests were performed with coal-derived flue gas to assess the performance of the individual components of the process as well as the combined overall benefits to the capture process from an initial parametric study which was followed by a long term study spanning ~1000 operating hours for evaluating long term system operability, stability of process components and performance. Process data were used as inputs for the EH&S assessment.

6.1 Facility Modification and Retrofit

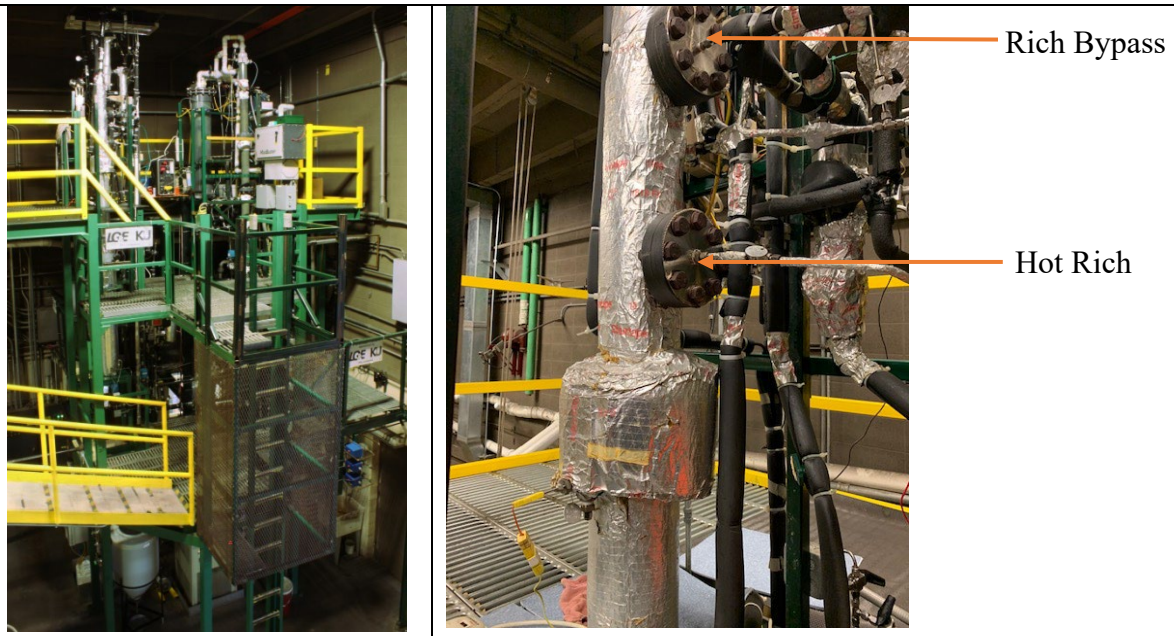

Exhibit 6.1.1. (a) Picture of 0.1 MWth CO_2 capture bench unit. (b) Stripper with two ports for split-flow streams.

The 0.1 MWth CO_2 capture bench unit shown in **Exhibit 6.1.1a**, consists of a 7.3 m (24 ft) tall by 10 cm (4") ID clear PVC absorber with a 25.4 cm (10") ID internally cooled storage tank at bottom, solvent recovery unit in the absorber exhaust stream, two stainless steel heat exchangers (a lean-rich heat exchanger for cross-flow heat recovery and a polisher for cooling of the CO_2-lean solution). The absorber has two sections of Flexipac 250Y with a packing height of 3.25 m. The unit has a stainless steel stripper that is 10 cm (4") ID in the upper tower section and 20 cm (8") ID in the lower reboiler section, and a condenser for solvent recovery in the stripper

exhaust. A hot-oil system and a chiller are installed to provide necessary heat for solvent regeneration and solution temperature control.

Split-Flow Modification and Retrofit

The flow of rich solvent through the lean-rich (L/R) heat exchanger was re-configured to allow two split streams to be directed to the stripper (the rich warm bypass is fed to the top and the hot stream to the upper mid-section of the packing) as shown in **Exhibit 6.1.1b** as a heat integration approach to lower the reboiler duty for solvent regeneration. Valves were added to direct flow and control the relative flow rates of the split streams to the stripper via an auto-control adjustable valve and two micro motion flow meters with pre-determined set points. To obtain desired temperature difference (10-15 °C) between the split flows, an additional existing heat exchanger was installed. A schematic of the modification with the additional heat exchanger and pictures of the insulated heat exchanger are shown in **Exhibits 6.1.2 and 6.1.3**.

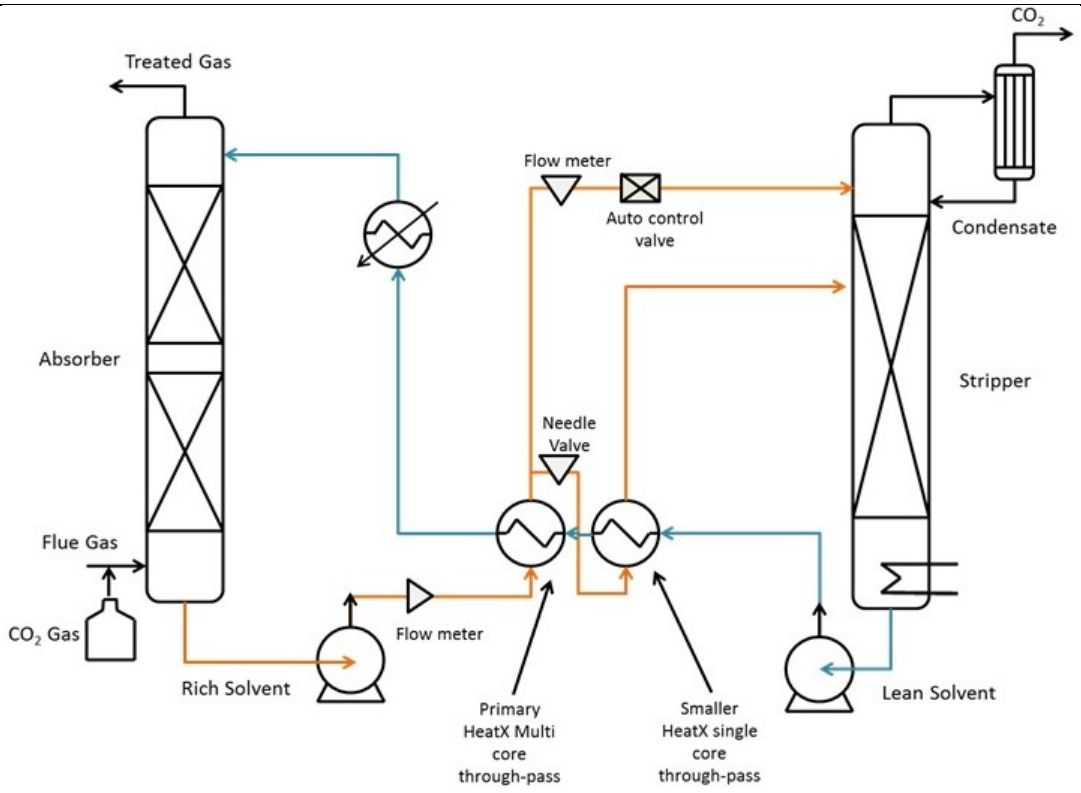

Exhibits 6.1.2. Process schematic for modification for split flow to stripper on 0.1 MWth unit.

Exhibits 6.1.3. Picture of insulated heat exchangers for split flow configuration in 0.1 MWth unit.

Heat Transfer Packing Installation

Design improvements to the heat transfer packing tested in the 3" bench unit were implemented by LNNL using an alternative pattern of heat transfer channels to increase the void space of the packing to ~88% compared to the <80% previously obtained. The 4" stainless steel printed heat transfer packing was installed in the 0.1 MWth bench unit with mounting supports to ensure proper load distribution from the integration of steel with the PVC absorber column. Sections of existing Flexipac 250Y packing at the top of the column were removed and replaced with two sections of the heat transfer packing material (1 ft height) as shown in **Exhibit 6.1.4.** Included are tubes for cooling water circulation for heat removal.

Exhibit 6.1.4. Picture of 4" stainless steel printed heat transfer packing material in 0.1 MWth unit.

6.2 Parametric Tests

6.2.1 Rich Stream Split-Flow to Stripper Evaluation

Experiments were performed at different split ratios (% of rich stream sent to the top of the stripper as warm stream) to determine conditions that maximized heat recovery in the stripper with resultant energy savings for the process. The split ratio was varied from 20 – 50% for different liquid circulation rates and carbon loading between 0.38-0.41 of C/N molar ratio in the rich stream exiting from the CO_2 absorber. With higher rich C/N, more energy savings are achieved. The best split flow conditions were compared with reference runs where the rich stream was fed to the stripper with no warm split.

Exhibit 6.2.1 is a summary of test conditions at split ratios of 20 – 40% for different liquid circulation rates (L/G of 3.2 – 3.6). For conditions 1-3, at an L/G of 3.2, the stripper bottom temperature was ~120 °C and the exhaust stripper temperature was ~100 °C. The benefit of the split feed is enhanced when with heat recovery between the warm and hot streams, lower stripper exhaust temperature is obtained. For condition 4, at a split ratio of 20%, the liquid circulation rate was increased (L/G = 3.6) and at a lower stripper bottom temperature, a reduction of the stripper exhaust temperature was obtained. With the lower stripper bottom temperature at ~116 °C and L/G of 3.4, the exhaust stripper temperature was further lowered. As observed for conditions 5 and 6 at the split ratio of 20% for the same solvent circulation rates, lowering the exhaust stripper temperature resulted in a lower energy of regeneration for comparable capture efficiency. At a lower stripper exhaust temperature, the amount of water vaporized per mole of CO_2 is lowered and therefore reduces the energy required for the process as shown by the estimated ratios of the partial pressures of water to CO_2, P_{H2O}/P_{CO2} in **Exhibit 6.2.1**. A comparison of condition 6 (with the lowest stripper top temperature) with a no split reference condition R, shows energy savings of up to ~15% could be realized with the rich stream split flow.

Exhibit 6.2.1. Test conditions for different split flow ratios of rich stream to stripper for varying liquid circulation rates.

	L/G	Split Flow (%)	% Capture	Stripper Bottom Temp (°C)	Stripper Top Temp (°C)	Lean Alkalinity (mol/kg)	Lean C/N	Rich C/N	PH_2O/PCO_2	Energy Btu/lb CO_2
1	3.2	20	64	120	99	6.50	0.23	0.36	1.45	1457
2	3.2	30	68	118	100	5.66	0.25	0.40	1.58	1570
3	3.2	40	69	118	101	5.21	0.23	0.37	1.74	1605
4	3.6	20	64	116	95	5.21	0.29	0.39	1.05	1322
5	3.4	20	74	117	93	4.93	0.28	0.40	0.90	1181
6	3.4	20	69	116	91	5.15	0.27	0.41	0.79	1080
R	3.4	0	68	117	99	5.50	0.28	0.39	1.45	1268

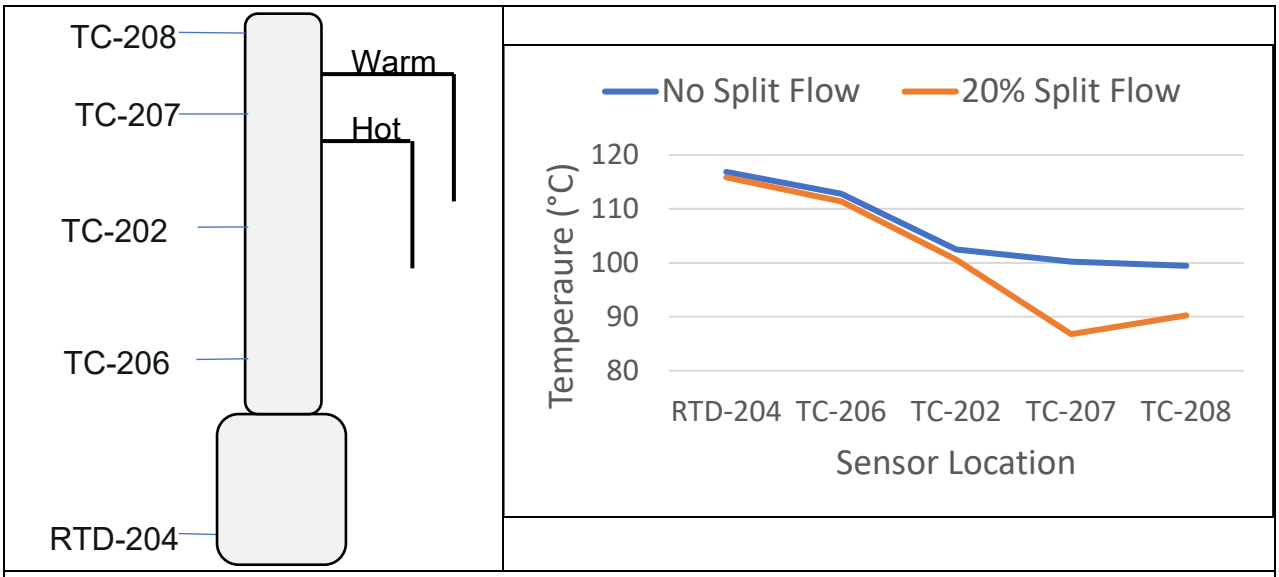

Exhibit 6.2.2. Schematic for temperature measurement locations on stripper and corresponding characteristic temperature profiles for experiment with and without rich solution split flows.

Using the test conditions at a split ratio of 20% with the lowest stripper exhaust temperature (condition 6), experiments were similarly performed with no split feed for comparison. **Exhibit 6.2.2** shows a schematic for the location of temperature measurement points with thermocouples (TC) and a resistance temperature detector (RTD) along the stripper and the corresponding temperature profiles obtained for the split and no split flow experiments. As shown, similar profiles were observed in the bottom section of the stripper but heat recovery from the split feed lowered temperatures in the upper section of the stripper resulting in a reduction of ~10 °C in the stripper exhaust temperature.

6.2.2 Heat Transfer Packing Evaluation

With the installation of two elements of the 6" tall 4" stainless steel printed heat transfer packing material between sections of the existing Flexipac 250Y packing of the absorber in the 0.1 MWth bench unit, experiments were conducted to evaluate its impact on process performance. The heat transfer packing is designed to be able to extract heat generated from the exothermic reaction of the solvent with the CO_2 absorbed. Circulating water to the packing material is used to cool the packing. The temperature of the water will therefore impact heat rejections and affect the temperature of the solvent in the absorber column and consequently its performance. Tests were performed at different circulating water temperatures (20 - 75 °C) to evaluate the impact of the heat transfer packing on the temperature profile and performance of the solvent. The water was circulated at 500 ml/min to each of the two sections of the heat transfer packing. **Exhibit 6.2.3** shows a schematic of the absorber and locations for thermocouples used to obtain the temperature profile shown for the different cooling water temperatures. A resistance temperature detector (RTD-270) measures the temperature of the lean solvent inlet to the top of the packing.

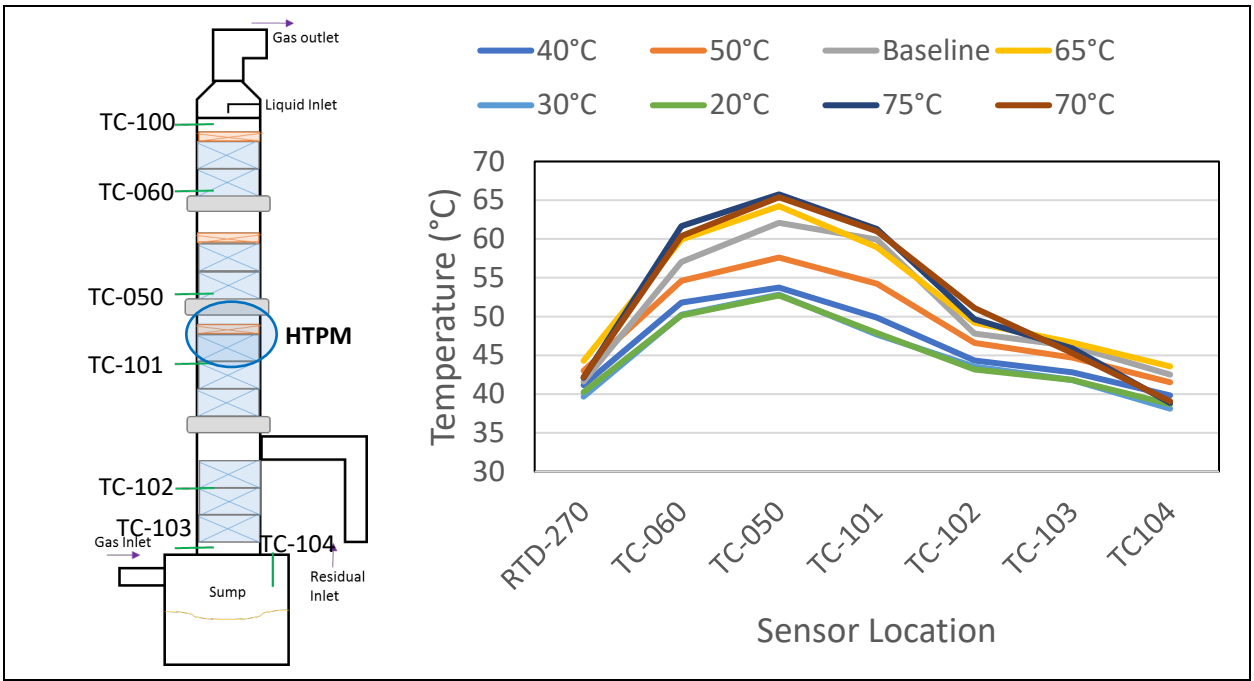

Exhibit 6.2.3. Schematic of temperature locations in absorber for the temperature profile obtained with the heat transfer packing material (HTPM) for circulating water temperature from (20 - 75 °C).

As shown in the figure, the bulge temperature for the solvent is located around TC-050 close to where the heat transfer packing material (HTPM) was installed. The baseline experiment (no cooling supplied to HTPM) showed a bulge temperature of ~62 °C. With circulating water temperatures from 20 - 50 °C the bulge temperature was lowered with corresponding lower temperatures down the column. For circulating water at higher temperatures, an increase in the bulge temperature was observed. The heat transfer packing was therefore used to tailor the bulge temperature as shown with the different circulating water temperatures. It is expected that the ability to lower the bulge temperature to reduce the flooding potential in a column of small diameter, along with the consequent temperature reduction of the solvent in the lower sections of the column, could enhance the rich loading. No significant enhancement in the rich loading, however, was observed from these tests. On the other hand, more liquid mal-distribution was observed at low-temperature circulating water flows through the HTPM. It was interpreted that the low packing surface temperature increased the solvent viscosity, contact angle and decreased the solvent surface tension. All of them could lead to severe liquid mal-distribution, particularly in a column with less than 8" diameter. To minimize the effect, a liquid redistributor is required. Experiments were also performed where a portion of the rich solvent was recirculated in the lower section of the absorber (pump around) to boost the rich loading and compared with similar test conditions without pump around. **Exhibit 6.2.4** shows a comparison of the temperature profile with and without pump around for different effects with the HTPM. With pump around (solid lines) to enhance the packing surface wetness, the temperatures of the solvent in the lower section of the absorber were higher than when there was no pump around, partially resulting from improved gas-liquid contact surface area for CO_2 capture at the bottom section of the absorber. Although no significant enhancement in rich loading was observed, using pump around reduced the energy of regeneration of the solvent compared to experiments without, as shown for the test conditions in **Exhibit 6.2.5**.

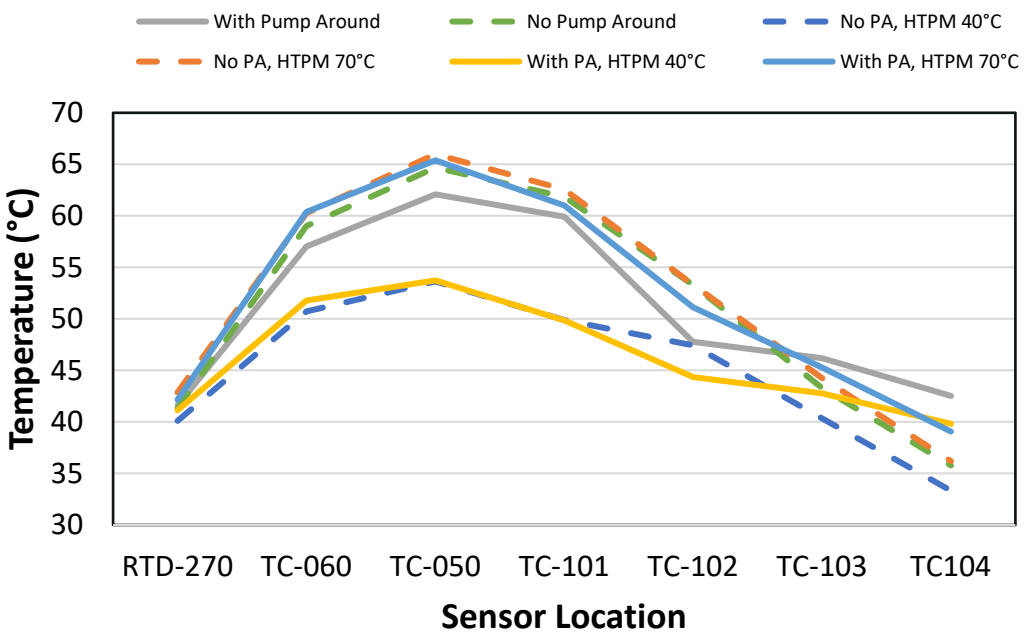

Exhibit 6.2.4. Temperature profile comparison for experiments with (solid lines) and without pump around (dashed lines) for heat transfer packing material evaluation for different cooling water conditions.

Exhibit 6.2.5. Effect of pump around on solvent performance with HTPM at different cooling water conditions.

		Split Flow % (Warm/Rich)	DP (inH_2O)	% Capture	Bulge Peak Temp (°C)	Energy Btu/lbCO_2	Lean Alkalinity (mol/kg)	Lean C/N	Rich C/N
No Pump Around	HTPM Off	20	2.8	62	65	1221	5.26	0.30	0.42
	HTPM 40C	20	2.5	59	54	1255	5.33	0.31	0.41
	HTPM 70C	20	2.7	60	66	1272	5.44	0.29	0.39
Pump Around	HTPM Off	20	3.5	69	62	1080	5.15	0.27	0.41
	HTPM 40C	20	4.1	67	54	1159	5.13	0.29	0.40
	HTPM 70C	20	2.5	64	65	1193	4.77	0.30	0.44

6.2.3 Zeolite Membrane Module Evaluation

Six membrane modules assembled by MPT which included 21 parts of 31-inch-long membrane tubes in each bundle (surface area 0.3 m^2) were evaluated in the 0.1 MWth bench unit. A QA/QC and stability test were conducted on the membrane modules to assess their performance prior to installation in the bench unit. A 70 wt% IPA/water solution was used for the dewatering test. The permeate water flux varied from 0.33 to 0.51 kg m^{-2} h^{-1} and rejection rates were above 97.8% as shown in **Exhibit 6.2.6**. For stability test with bundle C-03, a membrane flux of about 0.35 kg m^{-2} h^{-1} and rejection >97% were maintained for ~26 hr (**Exhibit 6.2.7**).

Exhibit 6.2.6. QA/QC test of six membrane bundles assembled by MPT.

Bundle ID	Test Temperature (°C)	Test Pressure (psig)	Water Content (wt%)	Water Flux (kg m^{-2} h^{-1})	IPA Rejection Rate (%)
Bundle C-02	88	20	30	0.33	98.5
Bundle C-03	88	20	28	0.38	97.8
Bundle C-07	88	23	25	0.44	99.4
Bundle C-08	88	22	25	0.41	98.3
Bundle C-09	88	22	25	0.43	99.2
Bundle C-10	88	22	27	0.51	99.1

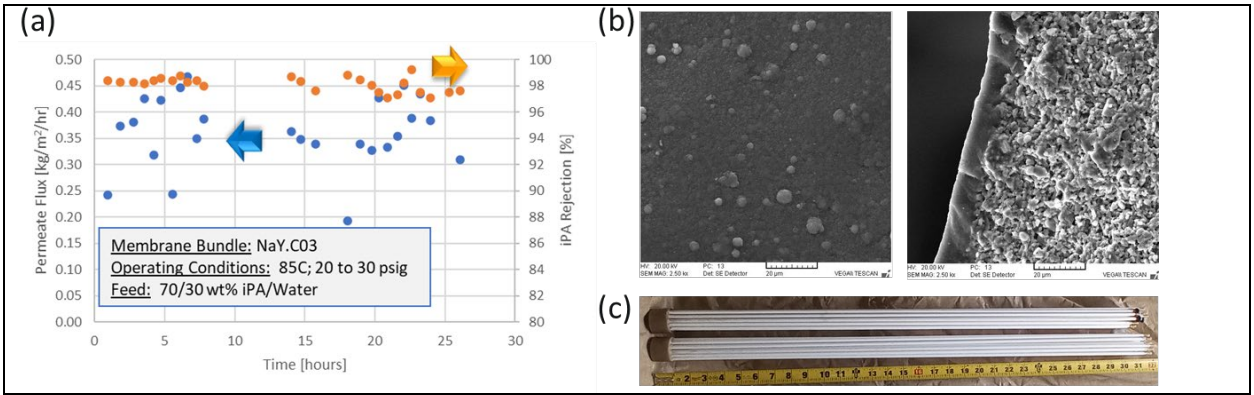

Exhibit 6.2.7 (a) Stability test of bundle C-03 in 70 wt% IPA/water at 88 °C, 22 psig (b) SEM image of membrane layer (c) membrane tubes in bundle.

The membrane bundles were installed in the 0.1 MWth bench unit and commissioned with CAER solvent using a warm rich split stream from the heat exchanger as feed solution at 80-85 °C. Initial temperature drop between inlet and outlet of the membrane system was ~20 °C. With improved insulation on valves, joints, and flanges as shown in **Exhibit 6.2.8**, the temperature drop between inlet and outlet of the membrane system dropped to ~10 °C. Membrane bundle #2 leaked after 40 minutes of testing due to tip damage. The other 5 membrane bundles were not leaking after 1 hour of operation. After commissioning, the membrane bundles were tested in the rich flow at 110 to 240 lb/hr. Membrane bundle #5 leaked after the first run. Membrane bundles 1, 3, 4 and 6 were tested at ~110 °C, 40 psig for a total of 33 hr with an average flux of 0.192 kg m^{-2} $h^{-1}$and rejection rate of 12.6%. Membrane bundle #6 also leaked afterward. Membrane bundles 1, 3 and 4 were

tested together at higher pressure 60-80 psig; the flux increased from 0.212 kg m^{-2} h^{-1} to 1.005 kg m^{-2} h^{-1} and rejection rate dropped from 20.1% to 5.7%. By testing these 3 membrane bundles separately, the same trend of degradation in membrane performance was observed. The dewatering test conditions and results are outlined in **Exhibit 6.2.9**. The leakages in the membrane modules and the observed under-performance precluded the projected benefits of membrane dewatering to the intensified process as a whole.

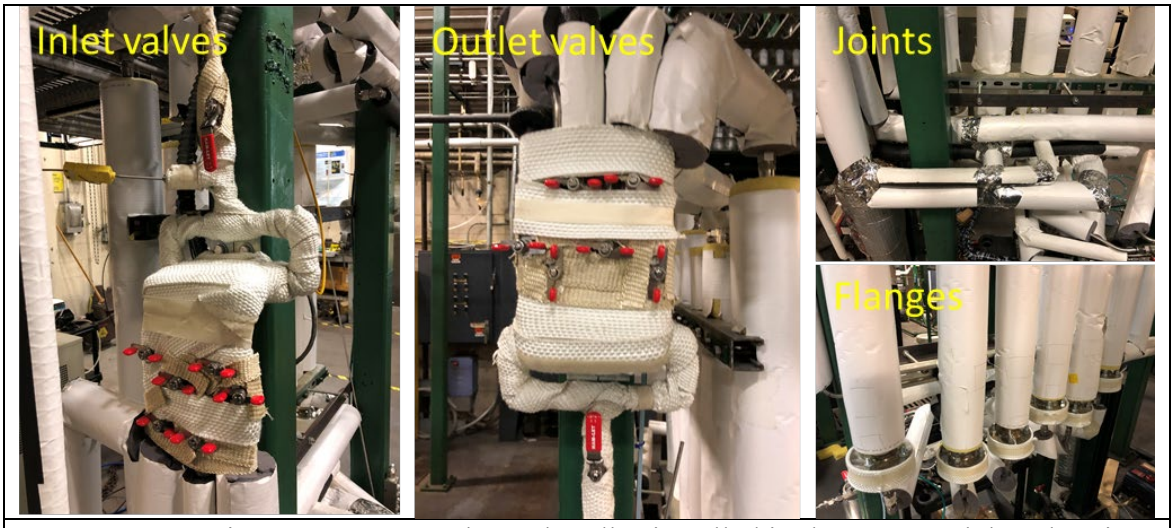

Exhibit 6.2.8. Six MPT NaY membrane bundles installed in the 0.1 MWth bench unit.

Exhibit 6.2.9. Dewatering test results of MPT NaY zeolite membrane bundles in CAER solvent.

Membrane Bundle	Run Time (Hour)	Pressure (psig)	Temp (inlet) (°C)	Temp (outlet) (°C)	Rich Flow (lb/hr)	Flux (kg m^{-2} h^{-1})	Rejection Rate (%)
1, 3, 4, 5, 6	6.42	40	112	90	114	0.036	10.2
1, 3, 4, 6	7.42	40	112	94	110	0.030	12.0
1, 3, 4, 6	5.42	40	112	96	130	0.059	12.1
1, 3, 4, 6	5.83	40	112	95	121	0.051	12.4
1, 3, 4, 6	5.73	40	104	100	242	0.122	13.4
1, 3, 4, 6	5.83	40	114	99	143	0.260	12.7
1, 3, 4, 6	2.97	40	110	101	200	0.630	12.9
1, 3, 4	2.08	80	109	100	240	0.212	17.4
1, 3, 4	0.80	60	111	92	114	0.444	20.1
1, 3, 4	0.42	80	104	95	197	1.005	5.7
1	5.67	80	114	104	180	0.061	55.3
1	1.417	80	104	96	200	0.034	42.3
3	1.33	80	109	103	217	0.236	29.2
3	0.167	80	105	96	200	1.098	22.9

4	3.30	80	112	104	233	0.344	13.7
4	0.250	80	105	96	200	1.563	7.6

Subsequent to the MPT membrane tests, the Hitachi membrane module (surface area of 0.3 m^2) was also installed and tested in the 0.1 MWth unit. Dewatering tests were performed at ~105-120 °C, 80 psig. Results are shown in **Exhibit 6.2.10.** The flux increased by about 150 times for tests at 120 °C compared to tests at 105 °C. The increased water solubility in the zeolite membrane with temperature increase contributed to the enhanced dewatering performance. For ~35hr duration of testing at 120 °C, the membrane flux increased from 0.536 kg m^{-2} h^{-1} to 1.449 kg m^{-2} h^{-1}, while rejection rate dropped from 82% to 40%. The decrease of rejection rate could be as a result of membrane fouling or degradation. The membrane was washed with DI water, ethanol/DI mixture followed by DI water again for 2 hours in each step to remove contaminants on the membrane surface and recover dewatering performance. Subsequent testing resulted in a significant increase of flux to 7.295 kg m^{-2} h^{-1} with the rejection rate decreasing to 30%. The membrane failed after total testing of ~82 hours.

Exhibit 6.2.10 Dewatering test results of Hitachi membrane bundle 1 in CAER solution.

Date	Run time (Hour)	Pressure (psig)	Temp (inlet) (°C)	Temp (outlet) (°C)	Rich Flow (lb/hr)	Flux (kg m^{-2} h^{-1})	Rejection Rate (%)
10/18/2021	5.3	60	104	94	190	0.009	11.58
10/21/2021	5.5	80	104	93	192	0.006	16.36
10/28/2021	2.7	80	104	94	190	0.030	31.90
10/28/2021	2.3	80	110	98	190	0.041	37.59
11/01/2021	4.2	80	111	99	190	0.056	66.56
11/02/2021	5.7	80	116	105	205	0.171	63.82
11/03/2021	4.9	80	116	104	191	0.202	70.55
11/04/2021	5.0	80	110	99	191	0.104	68.26
11/05/2021	6.0	80	105	94	191	0.046	38.20
11/08/2021	3.8	80	115	104	205	0.351	74.46
11/09/2021	6.0	80	120	107	190	0.536	81.83
11/15/2021	6.0	80	119	107	191	0.668	82.28
11/18/2021	5.2	80	119	107	190	0.972	75.84
11/19/2021	2.3	80	119	107	190	1.283	72.52
11/23/2021	6.3	80	119	107	190	1.283	61.07
11/24/2021	4.0	80	119	107	190	1.108	51.25
11/29/2021	4.8	80	119	107	190	1.449	40.00
12/09/2021	1.5	80	119	107	190	7.295	30.28

To further characterize the performance of the Hitachi membrane, a new bundle with 5 membranes (surface area = 0.25 m^2) was installed. Results for dewatering tests performed at 120 °C, 80 psig are shown in **Exhibit 6.2.11.** The membrane flux varied from 0.510 kg m^{-2} h^{-1} to 0.835 kg m^{-2} h^{-1}, while rejection rate dropped from 72.38% to 62.71%.

Exhibit 6.2.11 Dewatering test results of Hitachi membrane bundle 2 in CAER solution.

Date	Run time (Hour)	Pressure (psig)	Temp (inlet) (℃)	Temp (outlet) (℃)	Rich Flow (lb/hr)	Flux ($kg/m^2 \cdot h$)	Rejection Rate (%)
01/13/2022	8.3	80	119	107	190	0.510	70.98
01/20/2022	8.3	80	117	107	210	0.826	62.71
01/24/2022	7.5	80	117	106	210	0.835	69.41
01/27/2022	7.3	80	118	106	190	0.583	72.38

6.3 Long-Term Verification Studies

For the long-term solvent quality studies, the performance of the solvent was monitored over time for degradation and its impact on capture and energy of regeneration. To accelerate degradation, stripping conditions were chosen to expose the solvent to higher stripper bottom temperatures than what was used during the parametric studies (~116 °C). Higher stripper pressures of 28, 30 and 35 psia were tested increasing the stripper bottom temperatures to 121 – 125 °C. For these conditions, the warm split flow ratio of the rich solvent to the stripper was varied from 20 – 40% to determine conditions that provide reduced stripper exhaust temperatures to enhance the energy performance of the solvent. During these tests, the alkalinity of the solvent was monitored with solvent/water make-up added to maintain solvent concentration close to desired 5 mol/kg and periodic samples taken for degradation analysis. The solvent viscosity was also monitored to determine changes in its physical properties. **Exhibit 6.3.1** shows the long-term changes in viscosity, alkalinity, and solvent capacity of the solvent. There were no significant changes in the solvent properties during the tests. **Exhibit 6.3.2** shows representative results for the different stripping and split feed conditions.

Exhibit 6.3.3 shows solvent alkalinity and cyclic capacity of the solvent over an ~50 hour period for various operations in **Exhibit 6.3.2** to simulate the system fluctuation in the real world. With the capture efficiency of ~70% at set conditions for same liquid to gas ratios, and no significant changes in solvent alkalinity, the cyclic capacities observed compare well. With the observed energy performance of the solvent, the high pressure (30, 35 psia) at 40% split ratio was used mostly for the accelerated degradation for the latter part of the long-term operation. Representative performance with respect to capture and solvent capacity for the high stripper pressure runs are shown in **Exhibits 6.3.4** and **6.3.5** respectively. In the exhibits, the temperature difference between the stripper bottom temperature and the stripper top is represented by the delta temp. The results show that the solvent performance could be sustained over the long term. The sustained performance is further illustrated in **Exhibits 6.3.6** and **6.3.7** where the solvent performance was periodically monitored for the condition with split flow ratio of 20% and stripper pressure of 24

psia. Lower energy required for solvent regeneration corresponds to higher temperature difference between stripper top exhaust temperature and reboiler temperature, and higher carbon loading in the rich solution exiting absorber.

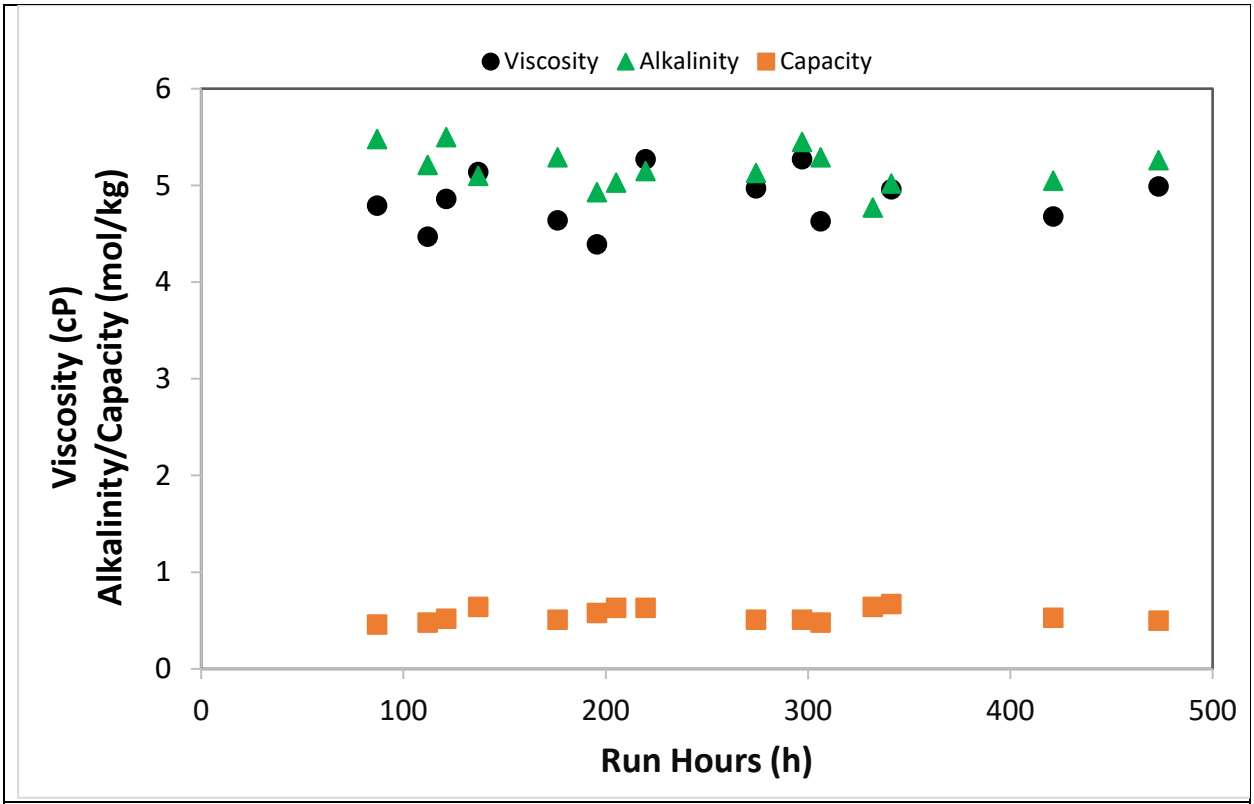

Exhibit 6.3.1. Solvent performance for different high temperature stripping conditions.

Exhibit 6.3.2. Solvent performance for different high temperature stripping conditions.

Condition	Solvent Lean Alkalinity (mol/kg)	Stripper Pressure (psia)	Stripper Bottom Temp. (°C)	Stripper Top Temp. (°C)	Split Feed Ratio (%Warm)	% Capture	Energy Btu/lb CO_2
1	5.17	28	121	95	20	74	1201
2	5.18	30	122	92	30	72	1152
3-1	5.15	30	122	91	40	70	1186
3-2	5.00	30	122	93	40	73	1208
3-3	5.19	30	122	92	40	69	1226
3-4	5.21	30	122	93	40	66	1285
3-5	5.10	30	122	92	40	68	1270
4-1	4.99	35	125	92	40	68	1155
4-2	5.21	35	125	94	40	69	1144
4-3	5.18	35	125	94	40	71	1179

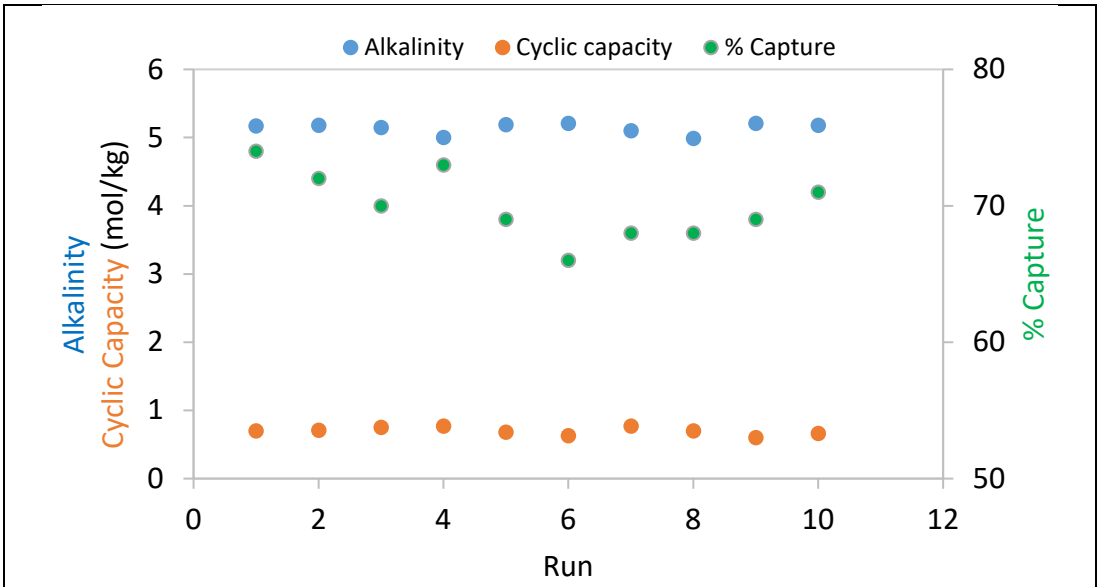

Exhibit 6.3.3. Solvent condition and performance for different high temperature stripping tests.

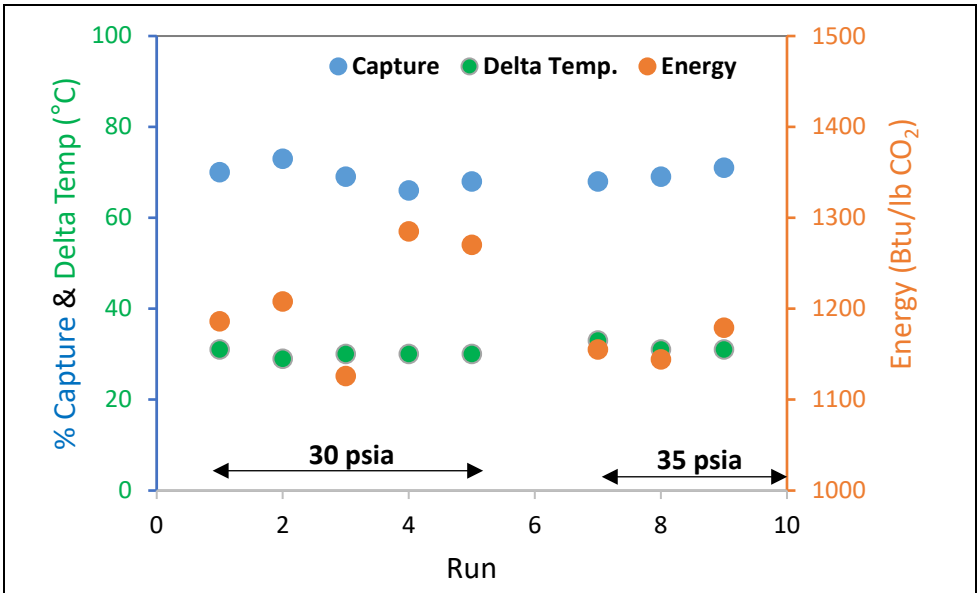

Exhibit 6.3.4. Solvent performance – capture efficiency and energy at stripper pressure of 30 and 35 psia with 40% split flow ratio.

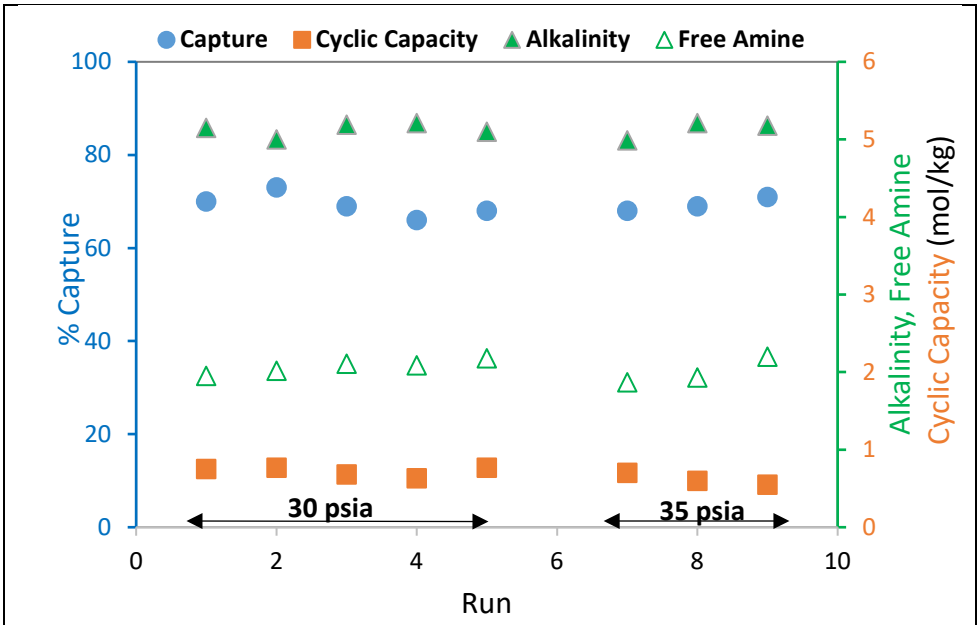

Exhibit 6.3.5. Solvent performance - conditions and loadings for stripping at 30 and 35 psia at 40% split flow ratio.

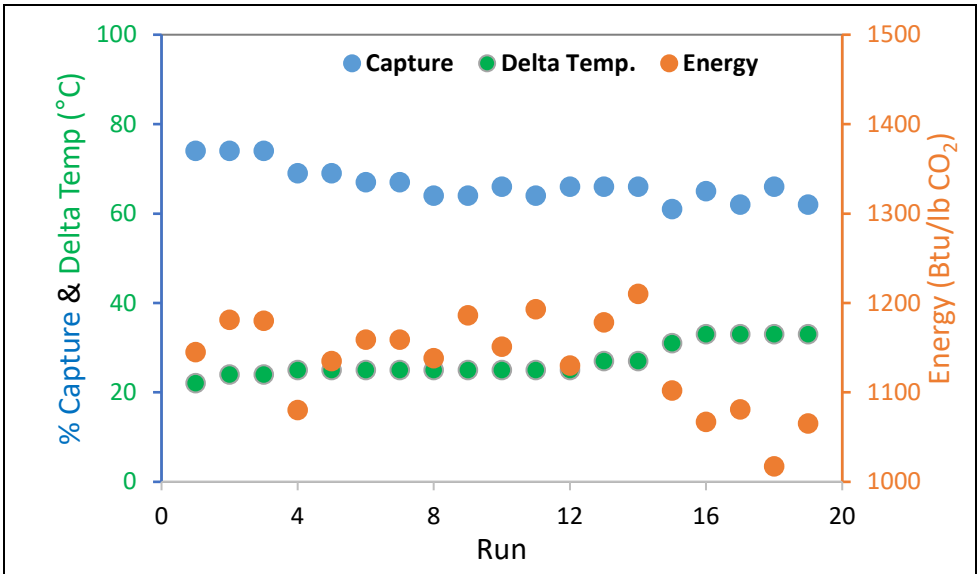

Exhibit 6.3.6. Long-term performance of solvent – capture and energy for 20% split flow ratio and stripping pressure of 24 psia.

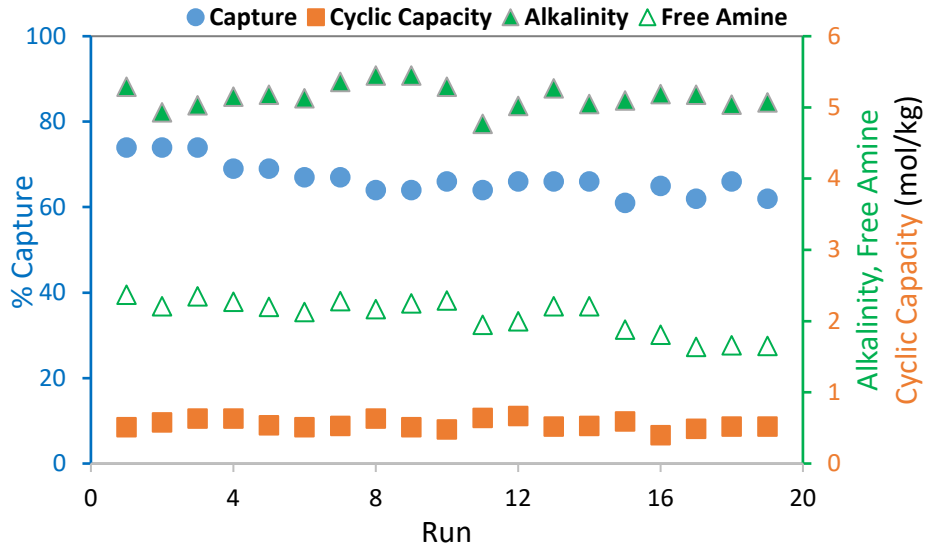

Exhibit 6.3.7. Long-term performance of solvent – capture and solvent loadings for 20% split flow ratio and stripping pressure of 24 psia.

7 SUMMARY OF TECHNO-ECONOMIC ANALYSIS

The techno-economic analysis (TEA) of UK CAER's technology was performed by Trimeric Corporation and submitted as a separate report (Sexton et al., January 27, 2022) to U.S. DOE NETL. For the analysis, the process configuration, process diagrams and heat and mass balance tables from ASPEN Plus were provided by UK CAER. The design basis which was comprised of technical inputs, economic inputs and system boundaries was made to correspond to the Department of Energy (DOE) established guidelines in its baseline report (DOE-NETL 2019). The process design and economic evaluation were based on a 650 MWe net plant.

The major components of the TEA included:

- A process overview and design basis for the commercial scale-up of the process,
- Process flow diagrams (PFD), stream tables, equipment lists, summaries of process heat duties and electric power requirements which served as a basis for the TEA,
- Estimation of energy performance for the CO_2 capture and compression system including power plant derating analysis,
- Equipment specification and sizing from stream table data,
- Capital and operating cost estimation, including identification of key cost centers,
- Comparison of energy performance, capital cost, cost of electricity, and cost of CO_2 capture to the DOE reference case (Case B12B) (DOE-NETL 2019).

The findings of the assessments are summarized below:
In comparison to the Case B12B, the UK CAER technology was shown to reduce the energy penalty, the levelized cost of electricity (LCOE) and the cost of CO_2 capture. The total parasitic demand was reduced by 11%; the increase in cost of electricity reduced by 16% while the cost of CO_2 capture also similarly lowered by 23%. The main driver for the reduction in cost of capture

was attributed to the capital cost savings (~44% reduction in total plant cost) that the UK CAER process offers compared to Case B12B. Even though the analysis showed a higher specific reboiler duty for the UK CAER process, the gross plant efficiency was improved from the heat recovery schemes employed in the process such as the superheat energy recovered from the steam extracted for the reboiler. Other additional process features which enhanced solvent energy performance included the:

(i) Novel in-situ cooling in the absorber to enhance solvent capacity,
(ii) Novel heat integration scheme that maximized heat recovery prior to solvent regeneration which reduced the steam required for regeneration,
(iii) Rich split feed to the primary stripper which maximized steam utilization. These energy improvements contributed to offset the increased specific reboiler duty to lower the overall parasitic demand of the capture process.

While these benefits are promising for the UK CAER technology, the analysis noted that optimizing heat integration networks as well as reduction in uncertainty in cost estimates for some process-specific equipment are pathways for further improvements in the process performance and economics of the UK CAER technology that can reduce risks and bolster prospect for further scaling. For example, future sensitivity analysis of the heat integration network to identify parts which provide most value and justification for the added capital cost and complexity would be worthwhile.

8 SUMMARY OF EH&S ASSESSMENT

The Environmental, Health and Safety (EH&S) assessment of UK CAER's intensified process was done by ALL4 LLC (formerly Smith Management Group) and submitted as a separate report (Whitney et al., Aug 2021) to U.S. DOE NETL. This was based on experimental data provided from the 0.1 MWth bench unit which was extrapolated for comparable evaluation of the impact on a commercial scale 650 MWnet coal-fired power plant.

The scope of the assessment was limited to evaluating process design plans, process operation and testing information provided by UK CAER as well as literature review. The literature review was performed to identify environmental, health and safety hazards of the raw materials used as well as available information for similar operations to evaluate potential air emissions, wastes and waste water generated. Chemical constituent evaluations were also done for known substances or those anticipated to be generated with the process. Process design and operation information included: process flow diagrams; operating parameters; raw material storage and consumption rates; air emissions testing; solvent testing; quantification and characterization of wastes generated and wastewater discharged. The technology was assessed for any unacceptable EH&S concerns that could prevent implementation both at the bench and commercial scales. An evaluation based on associated risks with hazardous chemicals, air emissions, waste-water discharges, solid-waste generated as well as employee hazards were considered. Findings of the report are summarized below.

No direct extremely hazardous substances (EHSs) were identified with the materials used in the process. Additional EHSs, incidental to the process identified, included ammonia, formaldehyde and two nitrosamines (N-nitrosodimethylamine and nitrosodimethylamine). The ammonia and formaldehyde are anticipated to be in the air emissions and require evaluation with releases beyond reporting thresholds. Nitrosamines were not identified in this bench-scale test and were not similarly detected in previous testing at UK CAER's 0.7 MWe small pilot unit at EW Brown Station in Harrodsburg, KY but further evaluation may be required if detected at a larger commercial facility.

Estimates for air emissions for the bench scale operation were well below threshold values considered relevant from air-permitting perspective. Estimates for regulated air emissions from raw material storage at commercial scale carbon capture system was shown to be minimal compared to the total air emissions from operation of a commercial scale post-combustion CO_2 capture system (PCCCS). The potential commercial scale air emissions for degradation products was estimated to be about 235 tons/year with the highest potential emitting degradation product being ammonia at about 175 tons/year. The assessment further indicated that from an air permitting perspective, the installation and operation of a 650 MWnet PCCCS at an existing fossil-fuel power plant would be subject to Potential for Significant Deterioration (PSD) for a regulated volatile organic compound (VOC) and New Source Review (NSR) requirements which would likely necessitate the installation of best available control technology (BACT) for the estimated increase in VOC emissions.

With respect to raw water usage, while this was minor in the bench-scale operations, it was estimated for a commercial scale PCCCS, an additional water demand of >50% could result compared to what is required for a plant without CO_2 control. This increased consumption comes with added considerations for reliable water source such as river, large reservoir or lake; commensurate water treatment requirements to remove solids, disinfect raw water and/or demineralization; and potential environmental permitting requirement for water withdrawal depending on the facility's water supply and how much it was already permitted to withdraw.

Waste water from the bench scale mainly from flue gas pretreatment (SO_2 removal prior to sending treated gas to process), cooling water use and make-up was relatively small. For a 650 MWnet commercial system, it was estimated that ~288,190 gallons per day of waste water will be generated with ~67% of the volume coming from flue gas pretreatment and the balance from cooling water blowdown. Routing waste water to the commercial facility waste water treatment system and re-using it as make-up for a power plant WFGD was identified as an ideal option which otherwise will require characterization of wastewater constituents and appropriate treatment for discharge through a National Pollutant Discharge Elimination System (NPDES) permit.

While no obvious concerns were identified for the bench unit operation and technology implementation at the commercial scale, it was noted that larger scale testing was required for better quantification of air emissions and potential formation of nitrosamines.

9 SUMMARY OF TECHNOLOGY GAP ANALYSIS

A Technology Gap Analysis (TGA) for solvent-based CO_2 capture technology was carried out as part of the project and submitted as a separate report (Frimpong et. al., February 23, 2022) to U.S. DOE NETL. The analysis identified the needs met by the various aspects of the technology evaluated in this project, the technology readiness levels and critical gaps that have to be bridged to further advance the technology. The major areas for consideration are summarized below:

In the absorption of CO_2 in the absorber where traditional structured packings are used to promote liquid-gas contact, enhanced mass transfer is obtained by increasing the liquid to gas interface which can be achieved by increasing the surface area the liquid flows across or increasing the wetting of the available surface. Generating additional surface area in the packing void space by forming discretized hill-shaped liquid films is also used to increase the liquid to gas interface. Design and construction methods for structured packing materials for increased surface areas such as the use of thin strips and deformed sheets, typically stainless steel material, come with inherent pressure drop challenges that need to be addressed. As the surface area is increased, the pressure drop also increases and the capacity, the ability to handle the liquid and gas flowrates, of the structured packing is decreased.

As demonstrated experimentally, the heat transfer packing with channels for cooling fluid can be used to tailor the bulge temperature in the upper section of the absorber where lowering of the bulge temperature results in enhanced mass transfer from the increased solubility of CO_2. However, the lower temperature increases the solvent viscosity which increases the contact angle and decreases wetting of the packing surface. This promotes liquid channel flow or maldistribution, reducing CO_2 absorption. A proper balance of the opposing phenomenon is therefore critical to ensure the benefit is maximized. The control of the bulge temperature provided by the heat transfer packing addresses the issue of under-utilized space of the absorber where traditionally majority of the reaction occurs in the top section. The modification of the temperature profile with the heat transfer packing would require reduced column heights resulting in reduced capital and operating costs. Some other research efforts include additively manufactured printed heat transfer packing at Oak Ridge National Laboratories for CO_2 capture and ION Engineering development of 3-D printed packing system that provide optimal gas-liquid contact, cooling, pressure drop, liquid hold-up and mass transfer.

The split rich feed to the stripper configuration employed by UK CAER minimizes water vapor lost with the exhaust gaseous stream common with traditional stripping and is one of various heat recovery approaches investigated by different researchers [Karimi et al. 2011, Le Moullec et al. 2014] to recover waste heat or latent heat in the CO_2 product vapor to ultimately lower the reboiler duty. Other forms of the technology are advanced with some being tested at pilot scale with verifiable benefits and energy savings [Knudsen et al. 2011, Mosey et al. 2011]. As shown in this project, and similarly reported in other studies for split flow configurations, it is critical the rich split ratio is optimized to maximize heat recovery to lower the solvent regeneration energy.

In UK CAER capture technology, a dewatering membrane (zeolite-based) for solvent enrichment prior to regeneration is used. Commercial reverse osmosis (RO), nanofiltration (NF) and ultrafiltration (UF) membranes have been investigated for enrichment of MEA solutions. UK

CAER in previous research examined commercially available RO membranes (polymer-based) for dewatering of its proprietary amine. While the RO membranes were able to accomplish dewatering of the amine-based solvent, the separation was performed at high pressure, high energy cost, and at room temperature. Since the implementation of the dewatering membrane will take place prior to the stripper, meaning temperature higher than 80 °C, the polymeric membranes would be unlikely to function. In addition, while stable for a few hours, the zeolite membranes were able to accomplish dewatering for extended time periods under relevant CO_2 capture process conditions. In commercial applications where dewatering is desired (such as lower carbon loadings present in natural gas CO_2 separation processes), these zeolite membranes may have some distinct advantages over other commercial options.

Some specific technology gaps identified include:

For heat transfer packing, (i) demonstration of a low-cost production method capable of producing parts without voids between the printed layers and with sufficient mechanical integrity to withstand operation; (ii) development and demonstration of a surface pattern or modification on the packing that overcomes low-temperature physical property changes of the solvent; and (iii) demonstration of larger scale application with connected smaller sections of manufactured packing, configured to function as one section.

As different stripper configurations increase process complexity, proper process controls of conditions and responses would be required to ensure smooth operations. While the benefits of many process configurations have been proposed, many of the efforts are based on simulations and more experimental validations as shown for the UK CAER split feed in this project are needed, particularly from scaled-up tests to advance the technologies. Scale up of cost effective, reproducible zeolite membranes is still a major challenge for zeolite membranes to compete with current state-of-the-art commercial polymeric membranes. Further developments of the zeolite membranes need to be pursued and scaled beyond what was demonstrated in the project for longer durations to establish sustained performance, stability and longevity to validate the technology.

10 TECHNOLOGY MATURATION PLAN

The technology maturation plan (TMP) initially submitted as a separate report (Landon J, July 2018) included a description of the technology readiness level (TRL) of the UK CAER technology, proposed work and highlights for moving the technology forward. The TRLs of the various technology aspects have since increased and updated based on validations from experimental tests performed on the UK CAER CCS bench units as summarized in Exhibit 10.1. The next phase to further increase the TRLs and advance these technologies would be projected scaled tests on UK CAER 0.7 MWe CCS unit, particularly for the split feed secondary vapor generation and heat transfer packing elements taking into consideration the necessary design adjustments and improvements needed. Market and deployment strategies will also be evaluated for commercial grade applications and cost benefits using existing relations with industrial collaborators and design firms.

Exhibit 10.1. Current TRLs of UK CAER CCS Transformation Elements and Technologies.					
	State of Technology		**Relevance of Validation Environment**		
UK CAER Element	**Current TRL**	**UK CAER Demonstration Scale**	**Characteristics of Commercial Scale Target**	**Level of Integration**	**Target Commercial Application(s)**
Zeolite Dewatering Membrane	6	Laboratory scale, 0.1 MWth CCS Bench Unit, Relevant solvents	Integrated into amine circulation loop, Real pulverized coal flue gas in capture system	Practical integration, dewatering under relevant process conditions	Fossil Fuel Power Generation Plants and other CO_2 Capture Applications, Water Recovery from High Concentration Brine
Heat Transfer Packing Material	5/6	Bench scale 3D printing, Laboratory scale, 0.1 MWth CCS Bench Unit, Relevant gas-liquid environment	High capacity and high efficiency packings evaluated, Temperature profiles monitored	Full Integration	Fossil Fuel Power Generation Plants and other CO_2 Capture Applications, Liquid Phase Adsorption Columns, Distillation
Secondary Vapor Generation in the Stripper	7	0.1 MWth CCS Bench Unit	Integration into solvent regeneration loop	Full Integration	Fossil Fuel Power Generation Plants and other CO_2 Capture Applications

11 CONCLUSION

The UK CAER technology for CO_2 capture which employs process intensification approaches to enhance solvent performance (improved absorption, enhanced rich loading) in the absorber with advanced heat transfer packing and maximizing heat recovery in the process with various process schemes (split-streams to the primary stripper, recovery of superheat from steam extracted from IP/LP steam from power cycle etc.) overall showed energy savings demonstrated experimentally and from the TEA. The TEA also showed significant capital cost reduction (~44% lower in overall plant cost) compared to the DOE reference Case B12B.

The advanced heat transfer packing tests on UK CAER CO_2 capture units (3" bench unit with simulated flue gas and 0.1 MWth unit with coal-derived flue gas) showed the bulge temperature in the absorber could be lowered by ~10 °C. The in-situ cooling provides a means to tailor the temperature profile to suit solvent properties to enhance absorption and increase its rich loading. As demonstrated on the 0.1 MWth unit, the split-flow of the rich stream to the stripper improved heat recovery during solvent regeneration lowering stripper exhaust temperatures by ~12 °C with resultant lowering of the regeneration energy by ~15%. Similar energy savings were shown from the TEA, where the UK CAER technology lowered the total parasitic demand by ~11% and associated cost of CO_2 capture by ~23%. The significant capital cost savings from UK CAER's capture unit itself, accounts for ~80% of the overall reduction in the cost of CO_2 capture compared with Case B12B as determined from the TEA. The high reboiler energy for the CAER process was offset by the process improvements leading to an overall improvement in gross plant efficiency. The EH&S assessment did not identify any direct extremely hazardous substances (EHSs) from the materials used in the process. Ammonia was noted as a major degradation product of the

solvent of interest from an air emissions perspective but no barriers were anticipated for deploying the technology at the commercial scale.

The improvements realized from the process intensification methods are generally solvent independent and further optimization would contribute to significant reductions in energy penalty, capital and operating costs in the CO_2 capture process.

12 LIST OF EXHIBITS

11 REFERENCES

DOE/NETL. "Cost and Performance Baseline for Fossil Energy Plants, Volume 1: Bituminous Coal and Natural Gas to Electricity." United States Department of Energy, September 2019.

Frimpong, R.; Irvin, B.; Zhu, F.; Nikolic, H.; Liu, K. "Technology Gap Analysis: A Process with Decoupled Absorber Kinetics and Solvent Regeneration through Membrane Dewatering and In-Column Heat Transfer." Submitted to DOE/NETL as part of work under Project DE-FE0031604. February 2022.

Sexton, A.; Fulk, S.; Jones, C.; Sachde, D. "Techno-Economic Analysis: A Process with Decoupled Absorber Kinetics and Solvent Regeneration through Membrane Dewatering and In-Column Heat Transfer." Submitted to DOE/NETL as part of work under Project DE-FE0031604. January 2022.

Whitney, C.; Konefal, N.; McCollam, S. "Environmental, Health and Safety Assessment: CO_2 Capture Process Using Decoupled Absorber Kinetics and Solvent Regeneration Through Membrane Dewatering." Submitted to DOE/NETL as part of work under Project DE-FE0031604. August 2021.

Karimi, M.; Hillestad, M.; Svendsen, H.F. Capital cost and energy considerations of alternative stripper configurations for post-combustion CO_2 capture. Chem. Eng. Res. Des. 2011, 89, 1229-1236.

Knudsen, J.N., Andersen J., Jensen, J.N., Biede O. Evaluation of process upgrades and novel solvents for the post-combustion CO_2 capture process in pilot scale. Energy Procedia 2011, 4, 1558-1565.

Landon, J. "Technology Maturation Plan: A Process with Decoupled Absorber Kinetics and Solvent Regeneration through Membrane Dewatering and In-Column Heat Transfer." Submitted to DOE/NETL as part of work under Project DE-FE0031604. July 2018.

Le Moullec, Y., Neveux, T., Al Azki, A.; Chikukwa, A.; Hoff, K.A. Process modifications for solvent-based PCCC. Int J. Greenhouse Gas Control 2014, 31, 96-112.

Liu, K.; Nikolic, H.; Thompson, J.; Frimpong, R.; Richburg, L. 2020. "Application of a Heat Integrated Post-combustion CO_2 Capture System with Hitachi Advanced Solvent into Existing Coal-Fired Power Plant." Submitted to U.S. Department of Energy National Energy Technology Laboratory. DOE/NETL Project DE-FE007395. June 2020.

Mosey, P.; Schmidt, S.; Sieder, G.; Garcia, H.; Stoffregen, T. Performance of MEA in a long-term test at the post-combustion capture pilot plant at Niederaussem. Int J. Greenhouse Gas Control 2011, 5, 620-627.

Zhou, J.; Zhou, C.; Xu, K.; Caro, J.; Huang, A. 2020. "Seeding-free synthesis of large tubular zeolite FAU membranes for dewatering carbonate by pervaporation." Microporous and Mesoporous Materials 292, 109713.

12 LIST OF ACRONYMS AND ABBREVIATIONS

3-D – Three-dimensional
ABS - Acrylonitrile Butadiene Styrene
BACT – Best Available Control Technology
C/N – Carbon to nitrogen Molar Ratio
CAER – Center for Applied Energy Research
CCS – CO_2 Capture System
DCC – Direct Contact Cooler
DI – Deionized
DMLS - Direct Metal Laser Sintering
DOE – U.S. Department of Energy
DPA – Discretized Packing Arrangement
EDS - Energy Dispersive X-ray Spectroscopy
EH&S – Environmental, Health and Safety
EHSs - Extremely Hazardous Substances
EPA - Environmental Protection Agency
HDPE – High Density Polyethylene
HTPM – Heat Transfer Packing Material
HXER – Heat Exchanger
FWH – Feed Water Heater
L/G – Liquid to Gas Mass Flow Ratio
LLNL - Lawrence Livermore National Laboratory
L/R – Lean/Rich
MEA – Monoethanolamine
MPT – Media Process & Technology
NEPA – National Environmental Policy Act
NETL – National Energy Technology Laboratory
NPDES - National Pollutant Discharge Elimination System
PCC – Post-combustion Capture
PFD – Process Flow Diagram
PMP – Project Management Plan
PS - Polystyrene
PSD - Prevention of Significant Deterioration
QA/QC – Quality Assurance/Quality Control
RTD – Resistance Temperature Device
SDS – Safety Data Sheet
SEM - Scanning Electron Microscopy
SLA - Sterolithography Apparatus
SMG – Smith Management Group
SS – Stainless Steel
TC - Thermocouple
TEA – Techno-economic Analysis
UK – University of Kentucky
VOC – Volatile Organic Compounds
WFGD – Wet Flue Gas Desulfurization

WWS – Water Wash System
XRD – X-ray diffraction